INTERNATIONAL JOURNAL OF
NUMERICAL ANALYSIS AND MODELING
Volume 22, Number 4, Pages 459–482

doi: 10.4208/ijnam2025-1020

ANALYSIS OF AN EFFICIENT PARAMETER UNIFORM DOMAIN DECOMPOSITION APPROACH FOR SINGULARLY PERTURBED GIERER-MEINHARDT TYPE NONLINEAR COUPLED SYSTEMS OF PARABOLIC PROBLEMS

AAKANSHA, SUNIL KUMAR, AND PRATIBHAMOY DAS

Abstract. This article presents an efficient domain decomposition algorithm of Schwarz waveform relaxation type for singularly perturbed Gierer-Meinhardt type nonlinear coupled systems of parabolic problems where the diffusion terms in each equation are multiplied by small parameters of different magnitudes. The magnitude of these small parameters leads to the sharpness and boundary layer behavior in the solution components. Our present algorithm considers a suitable decomposition of the domain and decouples the process of approximating the solution components at each time level. There are two different schemes proposed in this work. Specifically, the schemes use the backward Euler method combined with a suitable component-wise splitting for time discretization, while employing the central difference scheme for spatial discretization. The two numerical schemes differ in their splitting methods: Scheme 1 employs a Jacobi-type split, whereas Scheme 2 utilizes a Gauss-Seidel-type split. The exchange of information between neighboring subdomains is achieved through piecewise-linear interpolation. The convergence analysis of the algorithm is demonstrated using some auxiliary nonlinear systems. It is shown that the present procedure provides uniformly convergent numerical approximations to the solution having sharp spike components. Numerical experiments demonstrate that the considered algorithm with present discretization is more efficient in terms of accuracy and iteration counts than with the standard available approaches.

Key words. Schwarz waveform relaxation, domain decomposition method, Gierer-Meinhardt systems, singular perturbation, efficient algorithms, computational cost, CPU time.

1. Introduction

In the past two decades, analysis and simulation of coupled systems of parameterized nonlinear problems with boundary and interior layer phenomena have drawn the attention of physicists and applied mathematicians due to their numerous appearances inside the scientific community, see for e.g. nonlinear problems in [1, 2, 3, 4]. The computational analysis of these nonlinear PDE systems is not straightforward as it involves perturbation parameters of different magnitudes and coupling in the nonlinear terms [5, 6]. These problems are characterized by singularly perturbed problems when the arbitrary small perturbation parameters can not be approximated by zero. Gierer-Meinhardt model is one of the activator-inhibitor types of singularly perturbed nonlinear reaction diffusion system, which appears in pattern formation and morphogenesis and is of singularly perturbed multiple scale nature. Here, small diffusion of the activator and large diffusion of the inhibitor lead to sharp spike at the boundary points and make it of multiple-scale nature [7].

Veerman and Doleman [3] studied the existence and stability of localized pulses on the GM (Gierer-Meinhardt) equation with a slow nonlinearity, which can be

Received by the editors on February 23, 2024 and, accepted on January 24, 2025.
2000 *Mathematics Subject Classification.* 65M06, 65M12, 65M55.

formulated by the following multiple-scale reaction-diffusion equations

$$\begin{cases} \partial_t y_1 = \partial_x^2 y_1 + F(y_1, y_2), \\ \partial_t y_2 = \varepsilon^2 \partial_x^2 y_2 + G(y_1, y_2), \end{cases} \tag{1}$$

where $0 < \varepsilon \ll 1$ is a small parameter. A rigorous existence and stability analysis for GM equation corresponding to interior spike, boundary spike and two boundary spikes are examined in [8, 9] based on the boundary conditions. In general, the procedures of deriving wellposedness of a nonlinear problem use the fixed point theory, as given in [10].

Hence, we consider the following generalized version of nonlinear coupled system of GM equation for further behavior of its solutions and their computational efficiency, on $\Omega = \mathfrak{D} \times (0, \mathcal{T}]$, where $\mathfrak{D} = (0, 1)$:

$$\boldsymbol{\mathcal{L}}\boldsymbol{y} := \partial_t \boldsymbol{y}(x,t) - \boldsymbol{\varepsilon}\partial_x^2 \boldsymbol{y}(x,t) + \boldsymbol{f}(x,t,\boldsymbol{y}) = 0, \tag{2}$$

with initial and boundary conditions

$$\boldsymbol{y}(x,0) = \boldsymbol{\phi}(x),\ 0 \le x \le 1,$$

$$\boldsymbol{y}(0,t) = \boldsymbol{\varphi}_0(t),\ \boldsymbol{y}(1,t) = \boldsymbol{\varphi}_1(t),\ 0 < t \le \mathcal{T}.$$

Here, $\boldsymbol{\varepsilon} = diag(\varepsilon_1, \varepsilon_2)$ is a diagonal matrix such that the parameters ε_1 and ε_2 can have different magnitudes with $0 < \varepsilon_1 \le \varepsilon_2 \le 1$; $\boldsymbol{\mathcal{L}} = (\mathcal{L}_1, \mathcal{L}_2)^T$, the solution $\boldsymbol{y} = (y_1, y_2)^T$, the boundary data $\boldsymbol{\varphi} = (\varphi_1, \varphi_2)^T$, and initial data $\boldsymbol{\phi} = (\phi_1, \phi_2)^T$. We consider that the functions $\boldsymbol{f}, \boldsymbol{\phi}, \boldsymbol{\varphi}_0$, and $\boldsymbol{\varphi}_1$ are sufficiently smooth and appropriate compatibility conditions hold for the present problem, see [11]. Further, for all $(x, t, \boldsymbol{y}) \in \overline{\Omega} \times \mathbb{R}^2$, assume that the nonlinear reaction term $\boldsymbol{f} = (f_1, f_2)^T$ satisfies

$$\frac{\partial f_s}{\partial y_s}(x,t,y_1,y_2) \ge \overline{\alpha} > 0,\ \frac{\partial f_s}{\partial y_q}(x,t,y_1,y_2) \le 0,\ s \ne q,$$

$$\sum_{q=1}^{2} \frac{\partial f_s}{\partial y_q}(x,t,y_1,y_2) \ge \alpha > 0,\ s = 1, 2.$$

The investigation of multiple scale singularly perturbed problems became significantly important due to the rapid variation of continuous solutions in specific layer regions. Conventional simulators to solve such problems often encounter challenges in effectively handling sufficiently small diffusion terms. Consequently, the need arises for robust numerical methods to address these issues [12, 13]. Fitted/graded mesh [14, 15, 16, 17, 18, 19], fitted operator [20], and domain decomposition approaches are often used to construct such robust numerical algorithms for computational efficiency. This paper utilizes the domain decomposition approach, which is frequently used to reduce the computational cost, as like splitting approaches for coupled systems given in [21].

Domain decomposition approaches have gained significant popularity for effectively solving partial differential equations [22, 23, 24, 25, 26, 27]. Among these methods, Schwarz Waveform Relaxation (SWR) stands out as a special class specifically designed for time-dependent problems and was initially introduced in [29, 28]. The SWR approach involves dividing the original domain into space-time subproblems, where each subproblem is solved over the entire time window independently before exchanging interface data between subdomains. Notably, each subdomain can adopt its own space and time grid along with discretization techniques, making SWR highly adaptable and well-suited for parallel computing. SWR methods have been developed for a wide range of regular and singularly perturbed time-dependent

partial differential equations (where "regular" indicates non-singular perturbation nature) in [30, 31, 32, 23, 33, 34] and the references therein.

The research presented in [35, 36] delves into a semilinear system comprising two singularly perturbed parabolic reaction-diffusion equations set on a vertical strip. These equations contain highest order derivatives with divergent forms, which are multiplied by a small perturbation parameter ε^2. As the solution evolves, it reveals the existence of parabolic boundary layers of width $O(\varepsilon)$ in the vicinity of the strip boundary, particularly when ε approaches zero. In [35], the authors explore the condensing mesh method and the classical finite difference method as tools to construct a uniformly convergent difference scheme. On the other hand, [36] employs the integro-interpolation method to create a conservative nonlinear finite difference scheme, also demonstrating uniform convergence. In [11], a fitted mesh approach is considered for a semilinear system that involves two singularly perturbed parabolic reaction-diffusion equations with differing parameters. In [11], the discretization constituting the backward Euler scheme in time and the standard central differencing on Shishkin mesh in space is considered. So far, we are not aware of any paper that explored the utilization of the SWR approach to address the robust numerical solution of problem (2).

So, the purpose of the paper is two-fold: firstly, to develop an efficient SWR type domain decomposition method for solving problem (2), and secondly, to provide a comprehensive error analysis of the developed method. We define a suitable decomposition of the domain and decouple the process of approximating the solution's components at each time level. We develop two different schemes that use the backward Euler method combined with a suitable component-wise splitting for time discretization, while employing the central difference scheme for spatial discretization. Scheme 1 uses a Jacobi type split, while Scheme 2 uses a Gauss- Seidel type split. Following this, we introduce an iterative process, where the exchange of information between neighboring subdomains is achieved through piecewise-linear interpolation. The convergence analysis of the iterative process is demonstrated using some auxiliary problems. It is shown that the algorithm provides uniformly convergent numerical approximations to the solution. Numerical results demonstrate that the algorithm is more effective with the present discretization approach than the traditional discretization, which uses the backward Euler method on a uniform mesh in time and the usual central difference scheme on a uniform mesh in space.

The work is organized as follows. The continuous solution and its derivatives bounds are introduced in Section 2. In the section 3, we introduce a novel algorithm based on domain decomposition approach for solving the nonlinear system (2) by two proposed different schemes and analyze their convergence procedures in Section 4. Next, we give numerical experiments for a few Gierer-Meinhardt type systems in Section 5. Section 6 concludes the theoretical findings and provide the synopsis of the present convergence procedure.

Notation: The symbol $\boldsymbol{C}$ stands for a generic positive constant which is independent of perturbation parameters $\varepsilon_s, s = 1, 2$, the iteration parameter k and the number of partition points $\mathcal{N}$ and $\mathcal{M}$. $||.||_{L^\infty(J)}$ denotes the maximum norm, where J is a set which is both closed and bounded. $||.||_{L^\infty(J^{\mathcal{N},\mathcal{M}})}$ denotes the discrete maximum norm on the discrete domain $J^{\mathcal{N},\mathcal{M}}$ of J.

2. Analytical Properties of Singularly Perturbed Gierer-Meinhardt type Systems

We first recall the a priori derivative estimates for the solution of nonlinear system (2). The solution $\boldsymbol{y}$ of problem (2) is decomposed into $\boldsymbol{y} = \boldsymbol{v} + \boldsymbol{w}$. The solution components $\boldsymbol{v}$ and $\boldsymbol{w}$ denote the regular and singular parts of the solution $\boldsymbol{y}$ respectively, such that

$$\begin{cases} \partial_t \boldsymbol{v}(x,t) - \boldsymbol{\varepsilon}\partial_x^2 \boldsymbol{v}(x,t) + \boldsymbol{f}(x,t,\boldsymbol{v}) = \boldsymbol{0} \text{ in } \Omega, \\ \boldsymbol{v} = \boldsymbol{z} \text{ on } \{0,1\} \times (0,\mathcal{T}], \\ \boldsymbol{v} = \boldsymbol{\phi}(x) \text{ on } [0,1] \times \{0\}, \end{cases} \tag{3}$$

and

$$\begin{cases} \partial_t \boldsymbol{w}(x,t) - \boldsymbol{\varepsilon}\partial_x^2 \boldsymbol{w}(x,t) + \boldsymbol{f}(x,t,\boldsymbol{v}+\boldsymbol{w}) - \boldsymbol{f}(x,t,\boldsymbol{v}) = \boldsymbol{0} \text{ in } \Omega, \\ \boldsymbol{w} = \boldsymbol{y} - \boldsymbol{v} \text{ on } (\{0,1\} \times (0,\mathcal{T}]) \cup ([0,1] \times \{0\}), \end{cases} \tag{4}$$

where $\boldsymbol{z}$ satisfies

$$\begin{cases} \partial_t \boldsymbol{z} + \boldsymbol{f}(x,t,\boldsymbol{z}) = \boldsymbol{0}, \ (x,t) \in \{0,1\} \times (0,\mathcal{T}], \\ \boldsymbol{z}(x,0) = \boldsymbol{\phi}(x), \ x \in \{0,1\}. \end{cases} \tag{5}$$

Then, following the procedure in [11], we have

$$||\partial_t^s \boldsymbol{y}||_{L^\infty(\overline{\Omega})} \leq C, \ s = 0,1,2. \tag{6}$$

Further, the derivatives of the regular and singular parts of the solution are bounded as described in the following lemmas.

Lemma 2.1. *The regular part $v = (v_1, v_2)^t$ satisfies the following estimates*

$$||\partial_t^s \boldsymbol{v}||_{L^\infty(\overline{\Omega})} \leq C, \ ||\partial_x^s \boldsymbol{v}||_{L^\infty(\overline{\Omega})} \leq C, \ s = 0,1,2,$$

$$||\partial_x^s v_j||_{L^\infty(\overline{\Omega})} \leq C\varepsilon_j^{(1-s/2)}, \ j = 1,2; \ s = 3,4,$$

where C is independent of perturbation parameters $\varepsilon_s, s = 1,2$.

Proof. The proof follows using the arguments in Lemmas 4-6 of [11]. □

Lemma 2.2. *The singular part $w = (w_1, w_2)^t$ satisfies the following estimates*

$$|w_l(x,t)| \leq C\mathcal{B}_{\varepsilon_2}(x), \ l = 1,2,$$

$$|\partial_x^s w_1(x,t)| \leq C(\varepsilon_1^{-s/2}\mathcal{B}_{\varepsilon_1}(x) + \varepsilon_2^{-s/2}\mathcal{B}_{\varepsilon_2}(x)), \ |\partial_x^s w_2(x,t)| \leq C(\varepsilon_2^{-s/2}\mathcal{B}_{\varepsilon_2}(x)), \ s = 1,2,$$

$$|\partial_x^s w_1(x,t)| \leq C(\varepsilon_1^{-s/2}\mathcal{B}_{\varepsilon_1}(x) + \varepsilon_2^{-s/2}\mathcal{B}_{\varepsilon_2}(x)), \ s = 3,4,$$

$$|\partial_x^s w_2(x,t)| \leq C\varepsilon_2^{-1}(\varepsilon_1^{-(s-2)/2}\mathcal{B}_{\varepsilon_1}(x) + \varepsilon_2^{-(s-2)/2}\mathcal{B}_{\varepsilon_2}(x)), \ s = 3,4, \ \forall \ (x,t) \in \overline{\Omega}.$$

Further, for $\varepsilon_1 < \varepsilon_2$ and $\varepsilon_2 \leq \alpha/2$, the singular part $\boldsymbol{w} = (w_1, w_2)^T$ can be further decomposed as $w_1 = \hat{w}_{1,\varepsilon_1} + \hat{w}_{1,\varepsilon_2}$, $w_2 = \hat{w}_{2,\varepsilon_1} + \hat{w}_{2,\varepsilon_2}$, where

$$|\hat{w}_{1,\varepsilon_1}(x,t)| \leq \mathcal{B}_{\varepsilon_1}(x), \ |\partial_x^2 \hat{w}_{1,\varepsilon_1}(x,t)| \leq \varepsilon_1^{-1}\mathcal{B}_{\varepsilon_1}(x), \ |\partial_x^4 \hat{w}_{1,\varepsilon_2}(x,t)| \leq \varepsilon_2^{-2}\mathcal{B}_{\varepsilon_2}(x),$$
$$|\hat{w}_{2,\varepsilon_1}(x,t)| \leq \mathcal{B}_{\varepsilon_1}(x), \ |\partial_x^2 \hat{w}_{2,\varepsilon_1}(x,t)| \leq \varepsilon_2^{-1}\mathcal{B}_{\varepsilon_1}(x), \ |\partial_x^4 \hat{w}_{2,\varepsilon_2}(x,t)| \leq \varepsilon_2^{-2}\mathcal{B}_{\varepsilon_2}(x).$$

for $(x,t) \in \overline{\Omega}$. Here, C is independent of perturbation parameters $\varepsilon_s, s = 1,2$, and the layer functions $\mathcal{B}_{\varepsilon_q}(x)$ are defined as $\mathcal{B}_{\varepsilon_q}(x) = e^{-x\sqrt{\alpha/\varepsilon_q}} + e^{-(1-x)\sqrt{\alpha/\varepsilon_q}}$, $x \in [0,1], q = 1,2$.

Proof. The proof follows using the arguments in Lemmas 8,9, and 11 of [11]. □

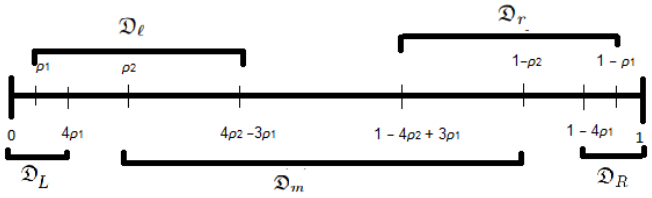

FIGURE 1. Decomposition in spatial direction.

3. Schwarz Waveform Relaxation Algorithm

From the derivative bounds given in the above lemmas, we can observe two overlapping boundary layers near the points $x = 0, 1$ where the derivative bounds are unbounded to the inverse powers of ε_n, $n = 1, 2$. These bounds lead to the non-convergence of the approximate solution on uniform meshes, if standard discretizations are used for continuous form of singularly perturbed Gierer-Meinhardt type systems. Here, a domain decomposition method is constructed to solve problem (2). The original domain is divided as follows: $\Omega_p = \mathfrak{D}_p \times \mathfrak{D}_t,\ p = L, \ell, m, r, R$, such that $\mathfrak{D}_L = (0, 4\rho_1),\ \mathfrak{D}_\ell = (\rho_1, 4\rho_2 - 3\rho_1),\ \mathfrak{D}_m = (\rho_2, 1-\rho_2),\ \mathfrak{D}_r = (1-4\rho_2 + 3\rho_1, 1-\rho_1),\ \mathfrak{D}_R = (1-4\rho_1, 1)$ and $\mathfrak{D}_t = (0, \mathcal{T}]$ (see Figure 1) with subdomain parameters ρ_1 and ρ_2 (see [37])

$$\rho_2 = \min\left\{\frac{4}{26},\ 2\sqrt{\frac{\varepsilon_2}{\alpha}}\ln\mathcal{N}\right\},\ \rho_1 = \min\left\{\frac{\rho_2}{4},\ 2\sqrt{\frac{\varepsilon_1}{\alpha}}\ln\mathcal{N}\right\}, \tag{7}$$

Here, the transition parameters are chosen in such a way that the subdomains $\mathfrak{D}_L$ and $\mathfrak{D}_R$ do not overlap with the subdomain $\mathfrak{D}_m$. On each subdomain $\Omega_p = \mathfrak{D}_p \times \mathfrak{D}_t$, we consider the mesh $\mathfrak{D}_p^{\mathcal{N}} \times \mathfrak{D}_t^{\mathcal{M}}$ defined as follows. For $\mathfrak{D}_p = (c, d)$, we define a mesh $\overline{\mathfrak{D}}_p^{\mathcal{N}} = \{x_i\}_{i=0}^{\mathcal{N}}$ with uniform step length $h_p = (d-c)/\mathcal{N}$, and the mesh $\overline{\mathfrak{D}}_t^{\mathcal{M}} = \{t_j\}_{j=0}^{\mathcal{M}}$ with uniform step length $\Delta t = \mathcal{T}/\mathcal{M}$ is defined on $\mathfrak{D}_t$. Suppose $\mathfrak{D}_p^{\mathcal{N}} = \overline{\mathfrak{D}}_p^{\mathcal{N}} \cap \mathfrak{D}_p$ and $\mathfrak{D}_t^{\mathcal{M}} = \overline{\mathfrak{D}}_t^{\mathcal{M}} \cap (0, \mathcal{T}]$. We consider the following discrete schemes on the subdomains $\Omega_p^{\mathcal{N},\mathcal{M}}$:

Scheme 1 :

$$[\boldsymbol{\mathcal{L}}_p^{\mathcal{N},\mathcal{M}}\mathbf{Y}_p]_{i,j} = \begin{pmatrix}[\mathcal{L}_{p,1}^{\mathcal{N},\mathcal{M}}\mathbf{Y}_p]_{i,j}\\ [\mathcal{L}_{p,2}^{\mathcal{N},\mathcal{M}}\mathbf{Y}_p]_{i,j}\end{pmatrix} = \mathbf{0}, \tag{8}$$

where

$$[\mathcal{L}_{p,1}^{\mathcal{N},\mathcal{M}}\mathbf{Y}_p]_{i,j} := [\delta_t^- Y_{p,1}]_{i,j} - \varepsilon_1[\delta_x^2 Y_{p,1}]_{i,j} + f_1(x_i, t_j, [Y_{p,1}]_{i,j}, [Y_{p,2}]_{i,j-1}) = 0,$$

$$[\mathcal{L}_{p,2}^{\mathcal{N},\mathcal{M}}\mathbf{Y}_p]_{i,j} := [\delta_t^- Y_{p,2}]_{i,j} - \varepsilon_2[\delta_x^2 Y_{p,2}]_{i,j} + f_2(x_i, t_j, [Y_{p,1}]_{i,j-1}, [Y_{p,2}]_{i,j}) = 0.$$

Scheme 2 :

$$[\boldsymbol{\mathcal{L}}_p^{\mathcal{N},\mathcal{M}}\mathbf{Y}_p]_{i,j} = \begin{pmatrix}[\mathcal{L}_{p,1}^{\mathcal{N},\mathcal{M}}\mathbf{Y}_p]_{i,j}\\ [\mathcal{L}_{p,2}^{\mathcal{N},\mathcal{M}}\mathbf{Y}_p]_{i,j}\end{pmatrix} = \mathbf{0}, \tag{9}$$

where

$$[\mathcal{L}_{p,1}^{\mathcal{N},\mathcal{M}}\mathbf{Y}_p]_{i,j} := [\delta_t^- Y_{p,1}]_{i,j} - \varepsilon_1[\delta_x^2 Y_{p,1}]_{i,j} + f_1(x_i, t_j, [Y_{p,1}]_{i,j}, [Y_{p,2}]_{i,j-1}) = 0,$$

$$[\mathcal{L}_{p,2}^{\mathcal{N},\mathcal{M}}\mathbf{Y}_p]_{i,j} := [\delta_t^- Y_{p,2}]_{i,j} - \varepsilon_2[\delta_x^2 Y_{p,2}]_{i,j} + f_2(x_i, t_j, [Y_{p,1}]_{i,j}, [Y_{p,2}]_{i,j}) = 0.$$

Here,

$$\delta_t^- \mathbf{W}_p(x_i,t_j) = \frac{\mathbf{W}_p(x_i,t_j) - \mathbf{W}_p(x_i,t_{j-1})}{\Delta t},$$

$$\delta_x^2 \mathbf{W}_p(x_i,t_j) = \frac{\mathbf{W}_p(x_{i-1},t_j) - 2\mathbf{W}_p(x_i,t_j) + \mathbf{W}_p(x_{i+1},t_j)}{h_p^2}.$$

Next, assuming $\overline{\Omega}^{\mathcal{N},\mathcal{M}} := (\overline{\Omega}_L^{\mathcal{N},\mathcal{M}} \backslash \overline{\Omega}_\ell) \cup (\overline{\Omega}_\ell^{\mathcal{N},\mathcal{M}} \backslash \overline{\Omega}_m) \cup \overline{\Omega}_m^{\mathcal{N},\mathcal{M}} \cup (\overline{\Omega}_r^{\mathcal{N},\mathcal{M}} \backslash \overline{\Omega}_m) \cup (\overline{\Omega}_R^{\mathcal{N},\mathcal{M}} \backslash \overline{\Omega}_r)$, and initial solution $\mathbf{Y}^0$ as

$$\begin{cases} \mathbf{Y}^0(x_i,t_j) = \mathbf{0} & \text{for } (x_i,t_j) \in \mathfrak{D} \times (0,\mathcal{T}], \\ \mathbf{Y}^0(x_i,t_j) = \boldsymbol{y}(x_i,t_j) & \text{for } (x_i,t_j) \in \overline{\mathfrak{D}}^{\mathcal{N}} \times \{0\}, \\ \mathbf{Y}^0(a,t_j) = \boldsymbol{y}(a,t_j) & \text{for } (a,t_j) \in \{0,1\} \times \mathfrak{D}_t^{\mathcal{M}}, \end{cases}$$

we calculate the numerical solution $\mathbf{Y}^k,\ k \geq 1$ of problem (2) on $\overline{\Omega}^{\mathcal{N},\mathcal{M}}$ as follows

$$\mathbf{Y}^k = \begin{cases} \mathbf{Y}_L^k \text{ in } \overline{\Omega}_L^{\mathcal{N},\mathcal{M}} \setminus \overline{\Omega}_\ell, \\ \mathbf{Y}_\ell^k \text{ in } \overline{\Omega}_\ell^{\mathcal{N},\mathcal{M}} \setminus \overline{\Omega}_m, \\ \mathbf{Y}_m^k \text{ in } \overline{\Omega}_m^{\mathcal{N},\mathcal{M}}, \\ \mathbf{Y}_r^k \text{ in } \overline{\Omega}_r^{\mathcal{N},\mathcal{M}} \setminus \overline{\Omega}_m, \\ \mathbf{Y}_R^k \text{ in } \overline{\Omega}_R^{\mathcal{N},\mathcal{M}} \setminus \overline{\Omega}_r, \end{cases} \tag{10}$$

where we solve

$$\begin{cases} [\boldsymbol{\mathcal{L}}_L^{\mathcal{N},\mathcal{M}} \mathbf{Y}_L^k]_{i,j} = \mathbf{0} \text{ in } \Omega_L^{\mathcal{N},\mathcal{M}}, \\ \mathbf{Y}_L^k(x_i,0) = \boldsymbol{\phi}(x_i) \text{ for } x_i \in \overline{\mathfrak{D}}_L^{\mathcal{N}}, \\ \mathbf{Y}_L^k(0,t_j) = \boldsymbol{\varphi}_0(t_j), \\ \mathbf{Y}_L^k(4\rho_1,t_j) = \mathcal{I}_j \mathbf{Y}^{k-1}(4\rho_1,t_j) \text{ for } t_j \in \mathfrak{D}_t^{\mathcal{M}}, \end{cases} \tag{11}$$

$$\begin{cases} [\boldsymbol{\mathcal{L}}_R^{\mathcal{N},\mathcal{M}} \mathbf{Y}_R^k]_{i,j} = \mathbf{0} \text{ in } \Omega_R^{\mathcal{N},\mathcal{M}}, \\ \mathbf{Y}_R^k(x_i,0) = \boldsymbol{\phi}(x_i) \text{ for } x_i \in \overline{\mathfrak{D}}_R^{\mathcal{N}}, \\ \mathbf{Y}_R^k(1-4\rho_1,t_j) = \mathcal{I}_j \mathbf{Y}^{k-1}(1-4\rho_1,t_j), \\ \mathbf{Y}_R^k(1,t_j) = \boldsymbol{\varphi}_1(t_j) \text{ for } t_j \in \mathfrak{D}_t^{\mathcal{M}}, \end{cases} \tag{12}$$

$$\begin{cases} [\boldsymbol{\mathcal{L}}_r^{\mathcal{N},\mathcal{M}} \mathbf{Y}_r^k]_{i,j} = \mathbf{0} \text{ in } \Omega_r^{\mathcal{N},\mathcal{M}}, \\ \mathbf{Y}_r^k(x_i,0) = \boldsymbol{\phi}(x_i) \text{ for } x_i \in \overline{\mathfrak{D}}_r^{\mathcal{N}}, \\ \mathbf{Y}_r^k(1-4\rho_2+3\rho_1,t_j) = \mathcal{I}_j \mathbf{Y}^{k-1}(1-4\rho_2+3\rho_1,t_j), \\ \mathbf{Y}_r^k(1-\rho_1,t_j) = \mathcal{I}_j \mathbf{Y}_R^k(1-\rho_1,t_j) \text{ for } t_j \in \mathfrak{D}_t^{\mathcal{M}}, \end{cases} \tag{13}$$

$$\begin{cases} [\boldsymbol{\mathcal{L}}_\ell^{\mathcal{N},\mathcal{M}} \mathbf{Y}_\ell^k]_{i,j} = \mathbf{0} \text{ in } \Omega_\ell^{\mathcal{N},\mathcal{M}}, \\ \mathbf{Y}_\ell^k(x_i,0) = \boldsymbol{\phi}(x_i) \text{ for } x_i \in \overline{\mathfrak{D}}_\ell^{\mathcal{N}}, \\ \mathbf{Y}_\ell^k(\rho_1,t_j) = \mathcal{I}_j \mathbf{Y}_L^k(\rho_1,t_j), \\ \mathbf{Y}_\ell^k(4\rho_2-3\rho_1,t_j) = \mathcal{I}_j \mathbf{Y}^{k-1}(4\rho_2-3\rho_1,t_j) \text{ for } t_j \in \mathfrak{D}_t^{\mathcal{M}}, \end{cases} \tag{14}$$

$$
(15)\qquad \begin{cases} [\boldsymbol{\mathcal{L}}_m^{\mathcal{N},\mathcal{M}}\mathbf{Y}_m^k]_{i,j} = \mathbf{0} \text{ in } \Omega_m^{\mathcal{N},\mathcal{M}}, \\ \mathbf{Y}_m^k(x_i,0) = \boldsymbol{\phi}(x_i) \text{ for } x_i \in \overline{\mathfrak{D}}_m^{\mathcal{N}}, \\ \mathbf{Y}_m^k(\rho_2,t_j) = \mathcal{I}_j\mathbf{Y}_\ell^k(\rho_2,t_j) \text{ for } t_j \in \mathfrak{D}_t^{\mathcal{M}}, \\ \mathbf{Y}_m^k(1-\rho_2,t_j) = \mathcal{I}_j\mathbf{Y}_r^k(1-\rho_2,t_j) \text{ for } t_j \in \mathfrak{D}_t^{\mathcal{M}}, \end{cases}
$$

where $\mathcal{I}_j\boldsymbol{Z}$ represents the piecewise linear interpolant of the discrete function $\boldsymbol{Z}$ at time level t_j. We repeat the process till $||\mathbf{Y}^{k+1} - \mathbf{Y}^k||_{L^\infty(\overline{\Omega}^{\mathcal{N},\mathcal{M}})} \leq \tau$ (user chosen parameter).

4. Convergence Analysis of the Algorithm

Here, we give convergence analysis of the proposed algorithm. We define some auxiliary problems and construct the mesh function $\widetilde{\mathbf{Y}}$ in a similar way as of (10). We define

$$
\begin{cases} [\boldsymbol{\mathcal{L}}_L^{\mathcal{N},\mathcal{M}}\widetilde{\mathbf{Y}}_L]_{i,j} = \mathbf{0} \text{ in } \Omega_L^{\mathcal{N},\mathcal{M}}, \\ \widetilde{\mathbf{Y}}_L(x_i,0) = \boldsymbol{\phi}(x_i) \text{ for } x_i \in \overline{\mathfrak{D}}_L^{\mathcal{N}}, \\ \widetilde{\mathbf{Y}}_L(0,t_j) = \boldsymbol{y}(0,t_j), \\ \widetilde{\mathbf{Y}}_L(4\rho_1,t_j) = \boldsymbol{y}(4\rho_1,t_j) \text{ for } t_j \in \mathfrak{D}_t^{\mathcal{M}}, \end{cases}
\qquad
\begin{cases} [\boldsymbol{\mathcal{L}}_R^{\mathcal{N},\mathcal{M}}\widetilde{\mathbf{Y}}_R]_{i,j} = \mathbf{0} \text{ in } \Omega_R^{\mathcal{N},\mathcal{M}}, \\ \widetilde{\mathbf{Y}}_R(x_i,0) = \boldsymbol{\phi}(x_i) \text{ for } x_i \in \overline{\mathfrak{D}}_R^{\mathcal{N}}, \\ \widetilde{\mathbf{Y}}_R(1-4\rho_1,t_j) = \boldsymbol{y}(1-4\rho_1,t_j), \\ \widetilde{\mathbf{Y}}_R(1,t_j) = \boldsymbol{y}(1,t_j) \text{ for } t_j \in \mathfrak{D}_t^{\mathcal{M}}, \end{cases}
$$

$$
\begin{cases} [\boldsymbol{\mathcal{L}}_r^{\mathcal{N},\mathcal{M}}\widetilde{\mathbf{Y}}_r]_{i,j} = \mathbf{0} \text{ in } \Omega_r^{\mathcal{N},\mathcal{M}}, \\ \widetilde{\mathbf{Y}}_r(x_i,0) = \boldsymbol{\phi}(x_i) \text{ for } x_i \in \overline{\mathfrak{D}}_r^{\mathcal{N}}, \\ \widetilde{\mathbf{Y}}_r(1-4\rho_2+3\rho_1,t_j) = \boldsymbol{y}(1-4\rho_2+3\rho_1,t_j), \\ \widetilde{\mathbf{Y}}_r(1-\rho_1,t_j) = \boldsymbol{y}(1-\rho_1,t_j) \text{ for } t_j \in \mathfrak{D}_t^{\mathcal{M}}, \end{cases}
$$

$$
\begin{cases} [\boldsymbol{\mathcal{L}}_\ell^{\mathcal{N},\mathcal{M}}\widetilde{\mathbf{Y}}_\ell]_{i,j} = \mathbf{0} \text{ in } \Omega_\ell^{\mathcal{N},\mathcal{M}}, \\ \widetilde{\mathbf{Y}}_\ell(x_i,0) = \boldsymbol{\phi}(x_i) \text{ for } x_i \in \overline{\mathfrak{D}}_\ell^{\mathcal{N}}, \\ \widetilde{\mathbf{Y}}_\ell(\rho_1,t_j) = \boldsymbol{y}(\rho_1,t_j), \\ \widetilde{\mathbf{Y}}_\ell(4\rho_2-3\rho_1,t_j) = \boldsymbol{y}(4\rho_2-3\rho_1,t_j) \text{ for } t_j \in \mathfrak{D}_t^{\mathcal{M}}, \end{cases}
$$

$$
\begin{cases} [\boldsymbol{\mathcal{L}}_m^{\mathcal{N},\mathcal{M}}\widetilde{\mathbf{Y}}_m]_{i,j} = \mathbf{0} \text{ in } \Omega_m^{\mathcal{N},\mathcal{M}}, \\ \widetilde{\mathbf{Y}}_m(x_i,0) = \boldsymbol{\phi}(x_i) \text{ for } x_i \in \overline{\mathfrak{D}}_m^{\mathcal{N}}, \\ \widetilde{\mathbf{Y}}_m(\rho_2,t_j) = \boldsymbol{y}(\rho_2,t_j), \\ \widetilde{\mathbf{Y}}_m(1-\rho_2,t_j) = \boldsymbol{y}(1-\rho_2,t_j) \text{ for } t_j \in \mathfrak{D}_t^{\mathcal{M}}. \end{cases}
$$

Here $\boldsymbol{\mathcal{L}}_p^{\mathcal{N},\mathcal{M}}, p = L,\ell,m,r,R$ are the discrete operators that were used in problems for $\mathbf{Y}_p^k, p = L,\ell,m,r,R$. The only difference between the problems for $\mathbf{Y}_p^k$ and $\widetilde{\mathbf{Y}}_p$ is in that we use the exact solution $\boldsymbol{y}$ of (2) in the boundary conditions for $\widetilde{\mathbf{Y}}_p, p = L,\ell,m,r,R$.

Now, using the solution $\widetilde{\mathbf{Y}}$ we split the global error $||\boldsymbol{y} - \mathbf{Y}^k||_{L^\infty(\overline{\Omega}^{\mathcal{N},\mathcal{M}})}$ into the discretization error $||\boldsymbol{y} - \widetilde{\mathbf{Y}}||_{L^\infty(\overline{\Omega}^{\mathcal{N},\mathcal{M}})}$ and iteration error $||\widetilde{\mathbf{Y}} - \mathbf{Y}^k||_{L^\infty(\overline{\Omega}^{\mathcal{N},\mathcal{M}})}$, and calculate the error bound by using the triangle inequality as follows

$$
(16)\qquad ||\boldsymbol{y} - \mathbf{Y}^k||_{L^\infty(\overline{\Omega}^{\mathcal{N},\mathcal{M}})} \leq ||\boldsymbol{y} - \widetilde{\mathbf{Y}}||_{L^\infty(\overline{\Omega}^{\mathcal{N},\mathcal{M}})} + ||\widetilde{\mathbf{Y}} - \mathbf{Y}^k||_{L^\infty(\overline{\Omega}^{\mathcal{N},\mathcal{M}})}.
$$

We will now separately bound each term on the right-hand side. We provide the details for Scheme 1 here, as Scheme 2 can be analyzed in a similar manner.

To bound the first term, we proceed as follows: consider Scheme 1 for $(x_i, t_j) \in \Omega_p^{\mathcal{N},\mathcal{M}}$, $p = L, \ell, m, r, R$. Then, for $n = 1, 2$, we have

$$\begin{aligned}
&[\delta_t^- e_{p,n}]_{i,j} - \varepsilon_n [\delta_x^2 e_{p,n}]_{i,j} \\
&+ (f_n(x_i, t_j, y_{n;i,j}, y_{3-n;i,j-1}) - f_n(x_i, t_j, \widetilde{Y}_{p,n;i,j}, \widetilde{Y}_{p,3-n;i,j-1})) \\
=&[(\delta_t - \partial_t) y_n]_{i,j} + \varepsilon_n [(\partial_x^2 - \delta_x^2) y_n]_{i,j} \\
&- (f_n(x_i, t_j, y_{n;i,j}, y_{3-n;i,j}) - f_n(x_i, t_j, y_{n;i,j}, y_{3-n;i,j-1})),
\end{aligned} \tag{17}$$

where $\mathbf{e}_p(x_i, t_j) = \boldsymbol{y}(x_i, t_j) - \widetilde{\mathbf{Y}}_p(x_i, t_j)$ denotes the error function and $\mathbf{e}_p = (e_{p,1}, e_{p,2})^T$. The error equation (17) can be defined as

$$\begin{aligned}
\mathscr{L}_{p,n}^{\mathcal{N},\mathcal{M}}(\boldsymbol{y} - \widetilde{\mathbf{Y}}_p)_{i,j} :=& [\delta_t^- e_{p,n}]_{i,j} - \varepsilon_n [\delta_x^2 e_{p,n}]_{i,j} + [s_{p,n}]_{i,j} (y_{1;i,j-n+1} - \widetilde{Y}_{p,1;i,j-n+1}) \\
&+ [q_{p,n}]_{i,j} (y_{2;i,j+n-2} - \widetilde{Y}_{p,2;i,j+n-2}) \\
=& [(\delta_t - \partial_t) y_n]_{i,j} + \varepsilon_n [(\partial_x^2 - \delta_x^2) y_n]_{i,j} \\
&- (f_n(x_i, t_j, y_{n;i,j}, y_{3-n;i,j}) - f_n(x_i, t_j, y_{n;i,j}, y_{3-n;i,j-1})),
\end{aligned}$$

where

$$\begin{aligned}
[s_{p,n}]_{i,j} = \int_0^1 \frac{\partial f_n}{\partial y_1} \Big(& x_i, t_j, \widetilde{Y}_{p,n;i,j} + a(y_{n;i,j} - \widetilde{Y}_{p,n;i,j}), \\
& \widetilde{Y}_{p,3-n;i,j-1} + a(y_{3-n;i,j-1} - \widetilde{Y}_{p,3-n;i,j-1}) \Big) \, da
\end{aligned}$$

and

$$\begin{aligned}
[q_{p,n}]_{i,j} = \int_0^1 \frac{\partial f_n}{\partial y_2} \Big(& x_i, t_j, \widetilde{Y}_{p,n;i,j} + a(y_{n;i,j} - \widetilde{Y}_{p,n;i,j}), \\
& \widetilde{Y}_{p,3-n;i,j-1} + a(y_{3-n;i,j-1} - \widetilde{Y}_{p,3-n;i,j-1}) \Big) \, da.
\end{aligned}$$

Now, using the mean-value theorem, the above expression leads to

$$\mathscr{L}_{p,n}^{\mathcal{N},\mathcal{M}}(\boldsymbol{y} - \widetilde{\mathbf{Y}}_p)_{i,j} = \left(\delta_t^- - \partial_t\right) y_{n;i,j} - \varepsilon_n \left(\delta_x^2 - \partial_x^2\right) y_{n;i,j} + a_n (y_{3-n;i,j} - y_{3-n;i,j-1}), \tag{18}$$

where $a_1 = \dfrac{\partial f_1}{\partial y_2}(x_i, t_j, \eta_{1;i,j}, \nu_{1;i,j})$, $a_2 = \dfrac{\partial f_2}{\partial y_1}(x_i, t_j, \eta_{2;i,j}, \nu_{2;i,j})$ and $\eta_{k;i,j}$, $\nu_{k;i,j}$, $k = 1, 2$, are intermediate values.

The operator $\mathscr{L}_p^{\mathcal{N},\mathcal{M}} = (\mathscr{L}_{p,1}^{\mathcal{N},\mathcal{M}}, \mathscr{L}_{p,2}^{\mathcal{N},\mathcal{M}})^T$ satisfies the following discrete maximum principle.

Lemma 4.1. *Suppose the mesh function $\boldsymbol{W}_p$ satisfies $\boldsymbol{W}_p(x_i, t_j) \geq \boldsymbol{0}$, $i = 0, \mathcal{N}$, $t_j \in \mathfrak{D}_t^{\mathcal{M}}$, and $\boldsymbol{W}_p(x_i, 0) \geq \boldsymbol{0}$ for $x_i \in \overline{\mathfrak{D}}_p^{\mathcal{N}}$. If $\mathscr{L}_p^{\mathcal{N},\mathcal{M}} \boldsymbol{W}_p \geq \boldsymbol{0}$ in $\Omega_p^{\mathcal{N},\mathcal{M}}$, then $\boldsymbol{W}_p \geq \boldsymbol{0}$ in $\overline{\Omega}_p^{\mathcal{N},\mathcal{M}}$.*

Proof. The lemma can be proved using the arguments in [11, Theorem 6]. □

Lemma 4.2. *Let $\boldsymbol{y}$ be the solution of (2) and $\widetilde{\mathbf{Y}}_p$ denote the solution of auxiliary problems defined above. Then*

$$||\boldsymbol{y} - \widetilde{\mathbf{Y}}_p||_{L^\infty(\overline{\Omega}_p^{\mathcal{N},\mathcal{M}})} \leq C(\mathcal{N}^{-2}(\ln \mathcal{N})^2 + \Delta t).$$

Proof. For the third term of equation (18), we have

$$\begin{aligned}
|a_n (y_{3-n;i,j} - y_{3-n;i,j-1})| &\leq C \, |(y_{3-n;i,j} - y_{3-n;i,j-1})| \\
&\leq C(t_j - t_{j-1}) \, \|\partial_t y_{3-n}(x_i, .)\|_{L^\infty([t_{j-1}, t_j])} \leq C\Delta t,
\end{aligned} \tag{19}$$

by using Taylor expansion and the derivative bound (6).

Further, for the first term of equation (18) we again use Taylor expansion and the derivative bound (6) to get

$$|\left(\delta_t^- - \partial_t\right) y_{n;i,j}| \leq C(t_j - t_{j-1}) \left\|\partial_t^2 y_n(x_i,.)\right\|_{L^\infty([t_{j-1},t_j])} \leq C\Delta t. \tag{20}$$

The estimation of the middle term of equation (18) depends on the subdomain. First, suppose $(x_i,t_j) \in \Omega_L^{\mathcal{N},\mathcal{M}}$. We will consider four different cases for ρ_1 and ρ_2 as follows.

Case 1: $\rho_2 = 4/26$ and $\rho_1 = \rho_2/4$.

In this case, the perturbation parameters are not very small. Further, we have $\varepsilon_1^{-1} \leq C\ln^2\mathcal{N}$, $\varepsilon_2^{-1} \leq C\ln^2\mathcal{N}$, and $h_L \leq C\mathcal{N}^{-1}$. Therefore, for $n = 1,2$, using Taylor expansions and bounds in Section 2 we get

$$\begin{aligned}\varepsilon_n \left|\left(\delta_x^2 - \partial_x^2\right) y_{n;i,j}\right| \leq & Ch_L^2\varepsilon_n \left\|\partial_x^4 y_n(.,t_j)\right\|_{L^\infty([x_{i-1},x_{i+1}])} \\ \leq & Ch_L^2(\varepsilon_1^{-1} + \varepsilon_2^{-1}) \leq C\mathcal{N}^{-2}(\ln\mathcal{N})^2.\end{aligned}$$

Case 2: $\rho_2 = 4/26$ and $\rho_1 = (2\sqrt{\varepsilon_1}\ln\mathcal{N})/\sqrt{\alpha}$.

In this case, we have $h_L \leq C\sqrt{\varepsilon_1}\mathcal{N}^{-1}\ln\mathcal{N}$. For $n = 1,2$, $\varepsilon_1 \leq \varepsilon_2$, Taylor expansions and bounds in Section 2 we get

$$\begin{aligned}\varepsilon_n \left|\left(\delta_x^2 - \partial_x^2\right) y_{n;i,j}\right| \leq & Ch_L^2\varepsilon_n \left\|\partial_x^4 y_n(.,t_j)\right\|_{L^\infty([x_{i-1},x_{i+1}])} \\ \leq & Ch_L^2(\varepsilon_1^{-1} + \varepsilon_2^{-1}) \leq C\mathcal{N}^{-2}(\ln\mathcal{N})^2.\end{aligned}$$

Case 3: $\rho_2 = (2\sqrt{\varepsilon_2}\ln\mathcal{N})/\sqrt{\alpha}$ and $\rho_1 = \rho_2/4$.

In this case, we have $h_L \leq C\sqrt{\varepsilon_2}\mathcal{N}^{-1}\ln\mathcal{N}$ and $\varepsilon_1^{-1/2} \leq 4\varepsilon_2^{-1/2}$. Thus, for $n = 1,2$, using Taylor expansions and bounds in Section 2 we have

$$\begin{aligned}\varepsilon_n \left|\left(\delta_x^2 - \partial_x^2\right) y_{n;i,j}\right| \leq & Ch_L^2\varepsilon_n \left\|\partial_x^4 y_n(.,t_j)\right\|_{L^\infty([x_{i-1},x_{i+1}])} \\ \leq & Ch_L^2(\varepsilon_1^{-1} + \varepsilon_2^{-1}) \leq C\mathcal{N}^{-2}(\ln\mathcal{N})^2.\end{aligned}$$

Case 4: $\rho_1 = (2\sqrt{\varepsilon_1}\ln\mathcal{N})/\sqrt{\alpha}$ and $\rho_2 = (2\sqrt{\varepsilon_2}\ln\mathcal{N})/\sqrt{\alpha}$.

In this case, ε_1 and ε_2 are the parameters of different magnitudes and they are small. We have $h_L \leq C\sqrt{\varepsilon_1}\mathcal{N}^{-1}\ln\mathcal{N}$. For $n = 1,2$, using Taylor expansions and bounds in Section 2 we obtain

$$\varepsilon_n \left|\left(\delta_x^2 - \partial_x^2\right) y_{n;i,j}\right| \leq Ch_L^2\varepsilon_n \left\|\partial_x^4 y_n(.,t_j)\right\|_{L^\infty([x_{i-1},x_{i+1}])} \leq C\mathcal{N}^{-2}(\ln\mathcal{N})^2.$$

Thus, combining the bounds in all four cases with the bounds (19)-(20) we get

$$|\mathscr{L}_{L,n}^{\mathcal{N},\mathcal{M}}(\boldsymbol{y} - \widetilde{\mathbf{Y}}_L)_{i,j}| \leq C(\mathcal{N}^{-2}(\ln\mathcal{N})^2 + \Delta t), n = 1,2, (x_i,t_j) \in \Omega_L^{\mathcal{N},\mathcal{M}}.$$

Hence, applying the discrete maximum principle for $\mathscr{L}_L^{\mathcal{N},\mathcal{M}}$ to $\boldsymbol{C}(\mathcal{N}^{-2}(\ln\mathcal{N})^2 + \Delta t) \pm (\boldsymbol{y} - \widetilde{\mathbf{Y}}_L)(x_i,t_j)$, we obtain

$$||\boldsymbol{y} - \widetilde{\mathbf{Y}}_L||_{L^\infty(\overline{\Omega}_L^{\mathcal{N},\mathcal{M}})} \leq C\mathcal{N}^{-2}(\ln\mathcal{N})^2 + C\Delta t.$$

Similarly,

$$||\boldsymbol{y} - \widetilde{\mathbf{Y}}_R||_{L^\infty(\overline{\Omega}_R^{\mathcal{N},\mathcal{M}})} \leq C\mathcal{N}^{-2}(\ln\mathcal{N})^2 + C\Delta t.$$

Next, for $(x_i,t_j) \in \Omega_\ell^{\mathcal{N},\mathcal{M}}$, $n = 1,2$, using (18) and (19)-(20) we have

$$|\mathscr{L}_{\ell,n}^{\mathcal{N},\mathcal{M}}(\boldsymbol{y} - \widetilde{\mathbf{Y}}_\ell)_{i,j}| \leq \varepsilon_n \left|\left(\delta_x^2 - \partial_x^2\right) y_{n;i,j}\right| + C\Delta t. \tag{21}$$

To calculate the estimate for $\varepsilon_n \left|\left(\delta_x^2 - \partial_x^2\right) y_{n;i,j}\right|$, we will make use of the decomposition $y_n = v_n + w_n$, $w_n = \hat{w}_{n,\varepsilon_1} + \hat{w}_{n,\varepsilon_2}$. We need to consider four different cases for ρ_1 and ρ_2 as follows.

Case 1: $\rho_2 = 4/26$ and $\rho_1 = \rho_2/4$.
Using arguments similar to those in Case 1 for $\Omega_L^{\mathcal{N},\mathcal{M}}$ we obtain

$$\varepsilon_n \left|\left(\delta_x^2 - \partial_x^2\right) y_{n;i,j}\right| \leq C\mathcal{N}^{-2}(\ln \mathcal{N})^2.$$

Case 2: $\rho_2 = 4/26$ and $\rho_1 = (2\sqrt{\varepsilon_1}\ln\mathcal{N})/\sqrt{\alpha}$.
In this case, $\varepsilon_2^{-1} \leq C\ln^2\mathcal{N}$, and $h_\ell \leq C\mathcal{N}^{-1}$. Using Taylor expansions and the derivative bounds in Section 2, for $n = 1, 2$, we get

$$\begin{aligned}
\varepsilon_n \left|\left(\delta_x^2 - \partial_x^2\right) y_{n;i,j}\right| &\leq Ch_\ell^2\varepsilon_n \left\|\partial_x^4 v_n(.,t_j)\right\|_{L^\infty([x_{i-1},x_{i+1}])} \\
&\quad + C\varepsilon_n \left\|\partial_x^2 \hat{w}_{n,\varepsilon_1}(.,t_j)\right\|_{L^\infty([x_{i-1},x_{i+1}])} \\
&\quad + Ch_\ell^2\varepsilon_n \left\|\partial_x^4 \hat{w}_{n,\varepsilon_2}(.,t_j)\right\|_{L^\infty([x_{i-1},x_{i+1}])} \\
&\leq C\mathcal{N}^{-2} + \|\mathcal{B}_{\varepsilon_1}\|_{L^\infty([x_{i-1},x_{i+1}])} + \mathcal{N}^{-2}(\ln\mathcal{N})^2 \\
&\leq C\mathcal{N}^{-2}(\ln\mathcal{N})^2.
\end{aligned}$$

Case 3: $\rho_2 = (2\sqrt{\varepsilon_2}\ln\mathcal{N})/\sqrt{\alpha}$ and $\rho_1 = \rho_2/4$.
Using arguments similar to those in Case 3 for $\Omega_L^{\mathcal{N},\mathcal{M}}$ we obtain

$$\varepsilon_n \left|\left(\delta_x^2 - \partial_x^2\right) y_{n;i,j}\right| \leq C\mathcal{N}^{-2}(\ln \mathcal{N})^2.$$

Case 4: $\rho_1 = (2\sqrt{\varepsilon_1}\ln\mathcal{N})/\sqrt{\alpha}$ and $\rho_2 = (2\sqrt{\varepsilon_2}\ln\mathcal{N})/\sqrt{\alpha}$
Using Taylor expansions and the derivative bounds in Section 2 with $h_\ell \leq C\sqrt{\varepsilon_1}\mathcal{N}^{-1}\ln\mathcal{N}$, we get

$$\begin{aligned}
\varepsilon_n \left|\left(\delta_x^2 - \partial_x^2\right) y_{n;i,j}\right| &\leq Ch_\ell^2\varepsilon_n \left\|\partial_x^4 v_n(.,t_j)\right\|_{L^\infty([x_{i-1},x_{i+1}])} \\
&\quad + C\varepsilon_n \left\|\partial_x^2 \hat{w}_{n,\varepsilon_1}(.,t_j)\right\|_{L^\infty([x_{i-1},x_{i+1}])} \\
&\quad + Ch_\ell^2\varepsilon_n \left\|\partial_x^4 \hat{w}_{n,\varepsilon_2}(.,t_j)\right\|_{L^\infty([x_{i-1},x_{i+1}])} \\
&\leq C\mathcal{N}^{-2} + \|\mathcal{B}_{\varepsilon_1}\|_{L^\infty([x_{i-1},x_{i+1}])} + \mathcal{N}^{-2}(\ln\mathcal{N})^2 \\
&\leq C\mathcal{N}^{-2}(\ln\mathcal{N})^2.
\end{aligned}$$

Now, applying the discrete maximum principle for $\mathscr{L}_\ell^{\mathcal{N},\mathcal{M}}$ to $\boldsymbol{C}(\mathcal{N}^{-2}(\ln\mathcal{N})^2 + \Delta t) \pm (\boldsymbol{y} - \widetilde{\mathbf{Y}}_\ell)(x_i, t_j)$, we obtain

$$||\boldsymbol{y} - \widetilde{\mathbf{Y}}_\ell||_{L^\infty(\overline{\Omega}_\ell^{\mathcal{N},\mathcal{M}})} \leq C\mathcal{N}^{-2}(\ln\mathcal{N})^2 + C\Delta t.$$

Similarly,

$$||\boldsymbol{y} - \widetilde{\mathbf{Y}}_r||_{L^\infty(\overline{\Omega}_r^{\mathcal{N},\mathcal{M}})} \leq C\mathcal{N}^{-2}(\ln\mathcal{N})^2 + C\Delta t.$$

Now, for $(x_i, t_j) \in \Omega_m^{\mathcal{N},\mathcal{M}}$, $n = 1, 2$, we use (18) and (19)-(20) to get

$$|\mathscr{L}_{m,n}^{\mathcal{N},\mathcal{M}}(\boldsymbol{y} - \widetilde{\mathbf{Y}}_m)_{i,j}| \leq \varepsilon_n \left|\left(\delta_x^2 - \partial_x^2\right) y_{n;i,j}\right| + C\Delta t. \tag{22}$$

To calculate the estimate for $\varepsilon_n \left|\left(\delta_x^2 - \partial_x^2\right) y_{n;i,j}\right|$, we proceed as follows.

Case 1: $\rho_2 = 4/26$ and $\rho_1 = \rho_2/4$
Using arguments similar to those in Case 1 for $\Omega_L^{\mathcal{N},\mathcal{M}}$ we obtain

$$\varepsilon_n \left|\left(\delta_x^2 - \partial_x^2\right) y_{n;i,j}\right| \leq C\mathcal{N}^{-2}(\ln \mathcal{N})^2.$$

Case 2: $\rho_2 = 4/26$ and $\rho_1 = (2\sqrt{\varepsilon_1}\ln\mathcal{N})/\sqrt{\alpha}$.
Using arguments similar to those in Case 2 for $\Omega_\ell^{\mathcal{N},\mathcal{M}}$ we obtain

$$\varepsilon_n \left|\left(\delta_x^2 - \partial_x^2\right) y_{n;i,j}\right| \leq C\mathcal{N}^{-2}(\ln \mathcal{N})^2.$$

Case 3: $\rho_2 = (2\sqrt{\varepsilon_2}\ln\mathcal{N})/\sqrt{\alpha}$ and $\rho_1 = \rho_2/4$; Case 4: $\rho_1 = (2\sqrt{\varepsilon_1}\ln\mathcal{N})/\sqrt{\alpha}$ and $\rho_2 = (2\sqrt{\varepsilon_2}\ln\mathcal{N})/\sqrt{\alpha}$.
For $n = 1, 2$, using the decomposition $y_n = v_n + w_n$, Taylor expansions, and bounds in Section 2 with $h_m \le C\mathcal{N}^{-1}$ we get

$$\begin{aligned}\varepsilon_n \left|\left(\delta_x^2 - \partial_x^2\right) y_{n;i,j}\right| \le & Ch_m^2\varepsilon_n \left\|\partial_x^4 v_n(.,t_j)\right\|_{L^\infty([x_{i-1},x_{i+1}])} \\ & + C\varepsilon_n \left\|\partial_x^2 w_n(.,t_j)\right\|_{L^\infty([x_{i-1},x_{i+1}])} \\ \le & C\mathcal{N}^{-2} + \|\mathcal{B}_{\varepsilon_2}\|_{L^\infty([x_{i-1},x_{i+1}])} \\ \le & C\mathcal{N}^{-2}.\end{aligned}$$

Now, applying the discrete maximum principle for $\mathscr{L}_m^{\mathcal{N},\mathcal{M}}$ to $\boldsymbol{C}(\mathcal{N}^{-2}(\ln\mathcal{N})^2 + \Delta t) \pm (\boldsymbol{y} - \widetilde{\mathbf{Y}}_m)(x_i, t_j)$, we obtain

$$||\boldsymbol{y} - \widetilde{\mathbf{Y}}_m||_{L^\infty(\overline{\Omega}_m^{\mathcal{N},\mathcal{M}})} \le C\mathcal{N}^{-2}(\ln\mathcal{N})^2 + C\Delta t.$$

We can establish the same bound for the Scheme 2 by applying the preceding arguments. □

Now, we will introduce a few notations that we will use in the further analysis.

$$\begin{aligned}\xi_{\rho_1} =& \max\{\max_{t_j\in\mathfrak{D}_t^{\mathcal{M}}} |(\widetilde{\mathbf{Y}}_\ell - \widetilde{\mathbf{Y}}_L)(\rho_1, t_j)|, \max_{t_j\in\mathfrak{D}_t^{\mathcal{M}}} |(\widetilde{\mathbf{Y}}_r - \widetilde{\mathbf{Y}}_R)(1-\rho_1, t_j)\},\\ \xi_{\rho_2} =& \max\{\max_{t_j\in\mathfrak{D}_t^{\mathcal{M}}} |(\widetilde{\mathbf{Y}}_m - \widetilde{\mathbf{Y}}_\ell)(\rho_2, t_j)|, \max_{t_j\in\mathfrak{D}_t^{\mathcal{M}}} |(\widetilde{\mathbf{Y}}_m - \widetilde{\mathbf{Y}}_r)(1-\rho_2, t_j)\},\\ \xi_{4\rho_1} =& \max\{\max_{t_j\in\mathfrak{D}_t^{\mathcal{M}}} |(\widetilde{\mathbf{Y}}_L - \mathcal{I}_j\widetilde{\mathbf{Y}}_\ell)(4\rho_1, t_j)|, \max_{t_j\in\mathfrak{D}_t^{\mathcal{M}}} |(\widetilde{\mathbf{Y}}_R - \mathcal{I}_j\widetilde{\mathbf{Y}}_r)(1-4\rho_1, t_j)\},\\ \xi_{4\rho_2-3\rho_1} =& \max\{\max_{t_j\in\mathfrak{D}_t^{\mathcal{M}}} |(\widetilde{\mathbf{Y}}_\ell - \mathcal{I}_j\widetilde{\mathbf{Y}}_m)(4\rho_2-3\rho_1, t_j)|,\\ & \max_{t_j\in\mathfrak{D}_t^{\mathcal{M}}} |(\widetilde{\mathbf{Y}}_r - \mathcal{I}_j\widetilde{\mathbf{Y}}_r)(1-4\rho_2+3\rho_1, t_j)\},\\ \xi^k =& \max\{\max_{t_j\in\mathfrak{D}_t^{\mathcal{M}}} |(\widetilde{\mathbf{Y}}_L - \mathcal{I}_j\mathbf{Y}^{k-1})(4\rho_1, t_j)|,\\ & \max_{t_j\in\mathfrak{D}_t^{\mathcal{M}}} |(\widetilde{\mathbf{Y}}_R - \mathcal{I}_j\mathbf{Y}^{k-1})(1-4\rho_1, t_j)|,\\ & \max_{t_j\in\mathfrak{D}_t^{\mathcal{M}}} |(\widetilde{\mathbf{Y}}_\ell - \mathcal{I}_j\mathbf{Y}^{k-1})(4\rho_2-3\rho_1, t_j)|,\\ & \max_{t_j\in\mathfrak{D}_t^{\mathcal{M}}} |(\widetilde{\mathbf{Y}}_r - \mathcal{I}_j\mathbf{Y}^{k-1})(1-4\rho_2+3\rho_1, t_j)|\},\end{aligned}$$

where ξ^k represents the iteration error, $\xi_{4\rho_1}$ and $\xi_{4\rho_2-3\rho_1}$ denote the interpolation errors, and ξ_{ρ_1} and ξ_{ρ_2} denote the discretization errors.

Now we proceed to bound the second term on the right hand side of (16). Here, we will discuss the proof for Scheme 1; the proof for Scheme 2 can be done analogously. For this purpose, we will introduce the operator $\mathbb{L}_p^{\mathcal{N},\mathcal{M}} = (\mathbb{L}_{p,1}^{\mathcal{N},\mathcal{M}}, \mathbb{L}_{p,2}^{\mathcal{N},\mathcal{M}})^T$ and then establish a discrete maximum principle for it.

Consider Scheme 1 for $(x_i, t_j) \in \Omega_p^{\mathcal{N},\mathcal{M}},\ p = L, \ell, m, r, R$. Then, the error equation of $\mathbf{e}_p^1(x_i, t_j) = (\widetilde{\mathbf{Y}}_p - \mathbf{Y}_p^1)$ is defined as

$$\begin{aligned}\mathbb{L}_{p,n}^{\mathcal{N},\mathcal{M}}(\widetilde{\mathbf{Y}}_p - \mathbf{Y}_p^1)_{i,j} :=& [\delta_t^- e_{p,n}^1]_{i,j} - \varepsilon_n[\delta_x^2 e_{p,n}^1]_{i,j} + [\hat{s}_{p,n}]_{i,j}(\widetilde{Y}_{1;i,j-n+1} - Y_{p,1;i,j-n+1}^1)\\ & + [\hat{q}_{p,n}]_{i,j}(\widetilde{Y}_{2;i,j+n-2} - Y_{p,2;i,j+n-2}^1) = 0,\ n = 1, 2,\end{aligned} \tag{23}$$

where

$$[\hat{s}_{p,n}]_{i,j} = \int_0^1 \frac{\partial f_n}{\partial y_1}\Big(x_i, t_j, Y^1_{p,n;i,j} + a(\widetilde{Y}_{n;i,j} - Y^1_{p,n;i,j}), \\ Y^1_{p,3-n;i,j-1} + a(\widetilde{Y}_{3-n;i,j-1} - Y^1_{p,3-n;i,j-1})\Big)\, da$$

and

$$[\hat{q}_{p,n}]_{i,j} = \int_0^1 \frac{\partial f_n}{\partial y_2}\Big(x_i, t_j, Y^1_{p,n;i,j} + a(\widetilde{Y}_{n;i,j} - Y^1_{p,n;i,j}), \\ Y^1_{p,3-n;i,j-1} + a(\widetilde{Y}_{3-n;i,j-1} - Y^1_{p,3-n;i,j-1})\Big)\, da.$$

Lemma 4.3. *Suppose the mesh function $\boldsymbol{Z}_p$ satisfies $\boldsymbol{Z}_p(x_i, t_j) \geq \boldsymbol{0},\ i = 0,\ \mathcal{N},$ $t_j \in \mathfrak{D}_t^{\mathcal{M}}$, and $\boldsymbol{Z}_p(x_i, 0) \geq \boldsymbol{0}$ for $x_i \in \overline{\mathfrak{D}}_p^{\mathcal{N}}$. If $\mathbb{L}_p^{\mathcal{N},\mathcal{M}} \boldsymbol{Z}_p \geq \boldsymbol{0}$ in $\Omega_p^{\mathcal{N},\mathcal{M}}$, then $\boldsymbol{Z}_p \geq \boldsymbol{0}$ in $\overline{\Omega}_p^{\mathcal{N},\mathcal{M}}$.*

Proof. The lemma can be proved using the arguments in [11, Theorem 6]. □

Theorem 4.4. *Suppose $\widetilde{\boldsymbol{Y}}$ and $\boldsymbol{Y}^k$ are the solutions of the auxiliary problems and the proposed algorithm respectively. Then*

$$||\widetilde{\boldsymbol{Y}} - \boldsymbol{Y}^k||_{L^\infty(\overline{\Omega}^{\mathcal{N},\mathcal{M}})} \leq C\left(\frac{1}{2}\right)^k + C(\mathcal{N}^{-2}(\ln \mathcal{N})^2 + \Delta t). \tag{24}$$

Proof. For $(x_i, t_j) \in \Omega_L^{\mathcal{N},\mathcal{M}}$, using (23), $\widetilde{\mathbf{Y}}_L - \mathbf{Y}_L^1$ satisfies

$$\mathbb{L}_L^{\mathcal{N},\mathcal{M}}(\widetilde{\mathbf{Y}}_L - \mathbf{Y}_L^1) = \mathbf{0},\ \text{in } \Omega_L^{\mathcal{N},\mathcal{M}},\ (\widetilde{\mathbf{Y}}_L - \mathbf{Y}_L^1)(x_i, 0) = \mathbf{0},\ x_i \in \overline{\mathfrak{D}}^{\mathcal{N}},$$
$$(\widetilde{\mathbf{Y}}_L - \mathbf{Y}_L^1)(0, t_j) = \mathbf{0},\ |(\widetilde{\mathbf{Y}}_L - \mathbf{Y}_L^1)(4\rho_1, t_j)| \leq \xi^1\mathbf{1},\ t_j \in \mathfrak{D}_t^M.$$

Assume the mesh function $\Psi_1^{\pm}(x_i, t_j) = \frac{x_i}{4\rho_1}\xi^1\mathbf{1} \pm (\widetilde{\mathbf{Y}}_L - \mathbf{Y}_L^1)(x_i, t_j)$ for $(x_i, t_j) \in \Omega_L^{\mathcal{N},\mathcal{M}}$. Now, employing the discrete maximum principle to the mesh function $\Psi_1^{\pm}(x_i, t_j)$, we obtain

$$|(\widetilde{\mathbf{Y}}_L - \mathbf{Y}_L^1)(x_i, t_j)| \leq \frac{x_i}{4\rho_1}\xi^1\mathbf{1},\ (x_i, t_j) \in \overline{\Omega}_L^{\mathcal{N},\mathcal{M}}.$$

For $(x_i, t_j) \in \overline{\Omega}_L^{\mathcal{N},\mathcal{M}} \backslash \overline{\Omega}_\ell$, $x_i \leq \rho_1$. Therefore

$$||\widetilde{\mathbf{Y}}_L - \mathbf{Y}_L^1||_{L^\infty(\overline{\Omega}_L^{\mathcal{N},\mathcal{M}} \backslash \overline{\Omega}_\ell)} \leq \frac{1}{4}\xi^1. \tag{25}$$

Similarly

$$||\widetilde{\mathbf{Y}}_R - \mathbf{Y}_R^1||_{L^\infty(\overline{\Omega}_R^{\mathcal{N},\mathcal{M}} \backslash \overline{\Omega}_r)} \leq \frac{1}{4}\xi^1. \tag{26}$$

Next, for $(x_i, t_j) \in \Omega_\ell^{\mathcal{N},\mathcal{M}},\ n = 1, 2$, using (23), the error equation of $\mathbf{e}_\ell^1(x_i, t_j) = (\widetilde{\mathbf{Y}}_\ell - \mathbf{Y}_\ell^1)$ is defined as

$$\mathbb{L}_{\ell,n}^{\mathcal{N},\mathcal{M}}(\widetilde{Y}_\ell - Y_\ell^1)_{i,j} := [\delta_t^- e^1_{\ell,n}]_{i,j} - \varepsilon_n[\delta_x^2 e^1_{\ell,n}]_{i,j} + [\hat{s}_{\ell,n}]_{i,j}(\widetilde{Y}_{1;i,j-n+1} - Y^1_{\ell,1;i,j-n+1}) \\ + [\hat{q}_{\ell,n}]_{i,j}(\widetilde{Y}_{2;i,j+n-2} - Y^1_{\ell,2;i,j+n-2}) = 0. \tag{27}$$

Thus, $\widetilde{\mathbf{Y}}_\ell - \mathbf{Y}_\ell^1$ satisfies

$$\mathbb{L}_\ell^{\mathcal{N},\mathcal{M}}(\widetilde{\mathbf{Y}}_\ell - \mathbf{Y}_\ell^1) = \mathbf{0},\ \text{in } \Omega_\ell^{\mathcal{N},\mathcal{M}},\ (\widetilde{\mathbf{Y}}_\ell - \mathbf{Y}_\ell^1)(x_i, 0) = \mathbf{0},\ x_i \in \overline{\mathfrak{D}}^{\mathcal{N}},$$
$$|(\widetilde{\mathbf{Y}}_\ell - \mathbf{Y}_\ell^1)(4\rho_2 - 3\rho_1, t_j)| \leq \xi^1\mathbf{1},\ t_j \in \mathfrak{D}_t^M,$$
$$|(\widetilde{\mathbf{Y}}_\ell - \mathbf{Y}_\ell^1)(\rho_1, t_j)| \leq |(\widetilde{\mathbf{Y}}_\ell - \widetilde{\mathbf{Y}}_L)(\rho_1, t_j)| + |(\widetilde{\mathbf{Y}}_L - \mathbf{Y}_\ell^1)(\rho_1, t_j)|$$

$$\leq \frac{1}{4}\xi^1\mathbf{1} + \xi_{\rho_1}\mathbf{1},\ t_j \in \mathfrak{D}_t^M.$$

Now, we consider mesh function $\Psi_2^{\pm}(x_i,t_j) = \zeta(x_i)\xi^1\mathbf{1} + \xi_{\rho_1}\mathbf{1} \pm (\widetilde{\mathbf{Y}}_\ell - \mathbf{Y}_\ell^1)(x_i,t_j)$ for $(x_i,t_j) \in \Omega_\ell^{\mathcal{N},\mathcal{M}}$, where $\zeta(x) = \dfrac{-x^2 + (13\rho_2 - 11\rho_1)x + 12\rho_2^2 + 24\rho_1^2 - 37\rho_1\rho_2}{48(\rho_2-\rho_1)^2}$, is an increasing function in the domain $[\rho_1, 4\rho_2 - 3\rho_1]$ with $\zeta(\rho_1) = 1/4$, $\zeta(4\rho_2 - 3\rho_1) = 1$, $\zeta(\rho_2) = 1/2$, $\zeta > 0$ in $\overline{\Omega}_\ell^{\mathcal{N},\mathcal{M}}$, and $\mathbb{L}_\ell^{\mathcal{N},\mathcal{M}}\zeta > 0$ in $\Omega_\ell^{\mathcal{N},\mathcal{M}}$. So, on employing the discrete maximum principle to the mesh function $\Psi_2^{\pm}(x_i,t_j)$ for $(x_i,t_j) \in \overline{\Omega}_\ell^{\mathcal{N},\mathcal{M}}$, we obtain

$$|(\widetilde{\mathbf{Y}}_\ell - \mathbf{Y}_\ell^1)(x_i,t_j)| \leq \zeta(x_i)\xi^1\mathbf{1} + \xi_{\rho_1}\mathbf{1}.$$

Therefore, we get

$$||\widetilde{\mathbf{Y}}_\ell - \mathbf{Y}_\ell^1||_{L^\infty(\overline{\Omega}_\ell^{\mathcal{N},\mathcal{M}}\setminus\overline{\Omega}_m)} \leq \frac{1}{2}\xi^1 + \xi_{\rho_1}. \tag{28}$$

Similarly

$$||\widetilde{\mathbf{Y}}_r - \mathbf{Y}_r^1||_{L^\infty(\overline{\Omega}_r^{\mathcal{N},\mathcal{M}}\setminus\overline{\Omega}_m)} \leq \frac{1}{2}\xi^1 + \xi_{\rho_1}. \tag{29}$$

Next, for $(x_i,t_j) \in \Omega_m^{\mathcal{N},\mathcal{M}},\ n = 1,2$, the error equation of $\mathbf{e}_m^1(x_i,t_j) = (\widetilde{\mathbf{Y}}_m - \mathbf{Y}_m^1)$ is defined as

$$\begin{aligned}\mathbb{L}_{m,n}^{\mathcal{N},\mathcal{M}}(\widetilde{Y}_m - Y_m^1)_{i,j} :=& [\delta_t^- e_{m,n}^1]_{i,j} - \varepsilon_n[\delta_x^2 e_{m,n}^1]_{i,j} + [\hat{s}_{m,n}]_{i,j}(\widetilde{Y}_{1;i,j-n+1} - Y_{m,1;i,j-n+1}^1)\\ &+ [\hat{q}_{m,n}]_{i,j}(\widetilde{Y}_{2;i,j+n-2} - Y_{m,2;i,j+n-2}^1) = 0.\end{aligned} \tag{30}$$

Thus, $\widetilde{\mathbf{Y}}_m - \mathbf{Y}_m^1$ satisfies

$$\mathbb{L}_m^{\mathcal{N},\mathcal{M}}(\widetilde{\mathbf{Y}}_\ell - \mathbf{Y}_m^1) = \mathbf{0},\ \text{in } \Omega_m^{\mathcal{N},\mathcal{M}},\ (\widetilde{\mathbf{Y}}_m - \mathbf{Y}_m^1)(x_i,0) = \mathbf{0},\ x_i \in \overline{\mathfrak{D}}^{\mathcal{N}},$$

$$\begin{aligned}|(\widetilde{\mathbf{Y}}_m - \mathbf{Y}_m^1)(\rho_2,t_j)| \leq& |(\widetilde{\mathbf{Y}}_m - \widetilde{\mathbf{Y}}_\ell)(\rho_2,t_j)| + |(\widetilde{\mathbf{Y}}_\ell - \mathbf{Y}_m^1)(\rho_2,t_j)|\\ \leq& \frac{1}{2}\xi^1\mathbf{1} + \xi_{\rho_1}\mathbf{1} + \xi_{\rho_2}\mathbf{1},\ t_j \in \mathfrak{D}_t^{\mathcal{M}}.\end{aligned}$$

$$\begin{aligned}|(\widetilde{\mathbf{Y}}_m - \mathbf{Y}_m^1)(1-\rho_2,t_j)| \leq& |(\widetilde{\mathbf{Y}}_m - \widetilde{\mathbf{Y}}_r)(1-\rho_2,t_j)| + |(\widetilde{\mathbf{Y}}_r - \mathbf{Y}_m^1)(1-\rho_2,t_j)|\\ \leq& \frac{1}{2}\xi^1\mathbf{1} + \xi_{\rho_1}\mathbf{1} + \xi_{\rho_2}\mathbf{1},\ t_j \in \mathfrak{D}_t^{\mathcal{M}}.\end{aligned}$$

Therefore, by employing the discrete maximum principle, we get

$$||\widetilde{\mathbf{Y}}_m - \mathbf{Y}_m^1||_{L^\infty(\overline{\Omega}_m^{\mathcal{N},\mathcal{M}})} \leq \frac{1}{2}\xi^1 + \xi_{\rho_1} + \xi_{\rho_2}. \tag{31}$$

Hence

$$||\widetilde{\mathbf{Y}} - \mathbf{Y}^1||_{L^\infty(\overline{\Omega}^{\mathcal{N},\mathcal{M}})} \leq \frac{1}{2}\xi^1 + \xi_{\rho_1} + \xi_{\rho_2}.$$

Now, we calculate the bound for the term $||\widetilde{\mathbf{Y}} - \mathbf{Y}^2||$. For this first we need to find the estimate for ξ^2. To this end we need to bound each term involved in the definition of ξ^2 separately.

Note that $\mathcal{I}_j\mathbf{Z}$ represents the piecewise linear interpolant of the mesh function $\mathbf{Z}$ at time level t_j. For any $x \in [x_{i-1}, x_i]$, it is defined as follows

$$\mathcal{I}_j\mathbf{Z}(x,t_j) = \frac{x_i - x}{x_i - x_{i-1}}\mathbf{Z}(x_{i-1,t_j}) + \frac{x - x_{i-1}}{x_i - x_{i-1}}\mathbf{Z}(x_i,t_j).$$

Hence, it is easy to deduce that

$$\begin{aligned}|\mathcal{I}_j\mathbf{Z}(x,t_j)| &\le \left|\frac{x_i-x}{x_i-x_{i-1}}\right||\mathbf{Z}(x_{i-1,t_j})| + \left|\frac{x-x_{i-1}}{x_i-x_{i-1}}\right||\mathbf{Z}(x_i,t_j)|\\ &\le \left(\frac{x_i-x}{x_i-x_{i-1}}+\frac{x-x_{i-1}}{x_i-x_{i-1}}\right)\max_{a\in\{x_i,x_{i-1}\}}|\mathbf{Z}(a,t_j)|\\ &= \max_{a\in\{x_i,x_{i-1}\}}|\mathbf{Z}(a,t_j)|.\end{aligned}$$

Using the triangle inequality, the operator $\mathcal{I}_j$ stability, and equation (28), we get

$$\begin{aligned}|(\widetilde{\mathbf{Y}}_L-\mathcal{I}_j\mathbf{Y}^1)(4\rho_1,t_j)| &\le |(\widetilde{\mathbf{Y}}_L-\mathcal{I}_j\widetilde{\mathbf{Y}}_\ell)(4\rho_1,t_j)| + |(\mathcal{I}_j\widetilde{\mathbf{Y}}_\ell-\mathcal{I}_j\mathbf{Y}^1)(4\rho_1,t_j)|\\ &\le \xi_{4\rho_1}\mathbf{1}+\frac{1}{2}\xi^1\mathbf{1}+\xi_{\rho_1}\mathbf{1}. \qquad (32)\end{aligned}$$

Similarly, applying the triangle inequality, the operator $\mathcal{I}_j$ stability, and equations (29) and (31), we obtain

$$\begin{aligned}&|(\widetilde{\mathbf{Y}}_R-\mathcal{I}_j\mathbf{Y}^1)(1-4\rho_1,t_j)|\\ \le&|(\widetilde{\mathbf{Y}}_R-\mathcal{I}_j\widetilde{\mathbf{Y}}_r)(1-4\rho_1,t_j)| + |(\mathcal{I}_j\widetilde{\mathbf{Y}}_r-\mathcal{I}_j\mathbf{Y}^1)(1-4\rho_1,t_j)|\\ \le&\xi_{4\rho_1}\mathbf{1}+\frac{1}{2}\xi^1\mathbf{1}+\xi_{\rho_1}\mathbf{1}, \qquad (33)\\ &|(\widetilde{\mathbf{Y}}_\ell-\mathcal{I}_j\mathbf{Y}^1)(4\rho_2-3\rho_1,t_j)|\\ \le&|(\widetilde{\mathbf{Y}}_\ell-\mathcal{I}_j\widetilde{\mathbf{Y}}_m)(4\rho_2-3\rho_1,t_j)| + |(\mathcal{I}_j\widetilde{\mathbf{Y}}_m-\mathcal{I}_j\mathbf{Y}^1)(4\rho_2-3\rho_1,t_j)|\\ \le&\xi_{4\rho_2-3\rho_1}\mathbf{1}+\frac{1}{2}\xi^1\mathbf{1}+\xi_{\rho_1}\mathbf{1}+\xi_{\rho_2}\mathbf{1}, \qquad (34)\\ &|(\widetilde{\mathbf{Y}}_r-\mathcal{I}_j\mathbf{Y}^1)(1-4\rho_2+3\rho_1,t_j)|\\ \le&|(\widetilde{\mathbf{Y}}_r-\mathcal{I}_j\widetilde{\mathbf{Y}}_m)(1-4\rho_2+3\rho_1,t_j)| + |(\mathcal{I}_j\widetilde{\mathbf{Y}}_m-\mathcal{I}_j\mathbf{Y}^1)(1-4\rho_2+3\rho_1,t_j))|\\ \le&\xi_{4\rho_2-3\rho_1}\mathbf{1}+\frac{1}{2}\xi^1\mathbf{1}+\xi_{\rho_1}\mathbf{1}+\xi_{\rho_2}\mathbf{1}. \qquad (35)\end{aligned}$$

Therefore, using the definition of ξ^2 and equations (32)-(35) we get

$$\xi^2 \le \frac{1}{2}\xi^1+\xi_{\rho_1}+\xi_{\rho_2}+\xi_{4\rho_1}+\xi_{4\rho_2-3\rho_1}.$$

Hence

$$\max\left\{\xi^2, ||\widetilde{\mathbf{Y}}-\mathbf{Y}^1||_{L^\infty(\overline{\Omega}^{\mathcal{N},\mathcal{M}})}\right\} \le \lambda+\frac{1}{2}\xi^1,\ \lambda=\xi_{\rho_1}+\xi_{\rho_2}+\xi_{4\rho_1}+\xi_{4\rho_2-3\rho_1}.$$

Utilizing the same arguments as before will lead to

$$\max\left\{\xi^{k+1}, ||\widetilde{\mathbf{Y}}-\mathbf{Y}^k||_{L^\infty(\overline{\Omega}^{\mathcal{N},\mathcal{M}})}\right\} \le \lambda+\frac{1}{2}\xi^k.$$

On simplifying the above expression, we get $\xi^k \le 2\lambda+\left(\frac{1}{2}\right)^{(k-1)}\xi^1$. Therefore,

$$||\widetilde{\mathbf{Y}}-\mathbf{Y}^k||_{L^\infty(\overline{\Omega}^{\mathcal{N},\mathcal{M}})} \le 2\lambda+\left(\frac{1}{2}\right)^k\xi^1. \qquad (36)$$

Since $\rho_1\in\overline{\mathfrak{D}}_L^{\mathcal{N}}$, $(1-\rho_1)\in\overline{\mathfrak{D}}_R^{\mathcal{N}}$, $\rho_2\in\overline{\mathfrak{D}}_\ell^{\mathcal{N}}$, $(1-\rho_2)\in\overline{\mathfrak{D}}_r^{\mathcal{N}}$, from Lemma 4.2, we have $\xi_{\rho_1}+\xi_{\rho_2}\le C(\mathcal{N}^{-2}(\ln\mathcal{N})^2+\Delta t)$.

To bound $\xi_{4\rho_1}$, we note that $|(\widetilde{\mathbf{Y}}_L-\mathcal{I}_j\widetilde{\mathbf{Y}}_\ell)(4\rho_1,t_j)| = |(\boldsymbol{y}-\mathcal{I}_j\widetilde{\mathbf{Y}}_\ell)(4\rho_1,t_j)|$ and $|(\widetilde{\mathbf{Y}}_R-\mathcal{I}_j\widetilde{\mathbf{Y}}_r)(1-4\rho_1,t_j)| = |(\boldsymbol{y}-\mathcal{I}_j\widetilde{\mathbf{Y}}_r)(1-4\rho_1,t_j)|$. We now provide details to

bound $|(\boldsymbol{y}-\mathcal{I}_j\widetilde{\mathbf{Y}}_\ell)(4\rho_1,t_j)|$; similarly, one can obtain the same bound for $|(\boldsymbol{y}-\mathcal{I}_j\widetilde{\mathbf{Y}}_r)(1-4\rho_1,t_j)|$. Using the triangle inequality we have

$$|(\boldsymbol{y}-\mathcal{I}_j\widetilde{\mathbf{Y}}_\ell)(4\rho_1,t_j)| \le |(\boldsymbol{y}-\mathcal{I}_j\boldsymbol{y})(4\rho_1,t_j)| + |\mathcal{I}_j(\boldsymbol{y}-\widetilde{\mathbf{Y}}_\ell)(4\rho_1,t_j)|. \tag{37}$$

Using stability of $\mathcal{I}_j$ and Lemma 4.2, we get

$$|\mathcal{I}_j(\boldsymbol{y}-\widetilde{\mathbf{Y}}_\ell)(4\rho_1,t_j)| \le C(\mathcal{N}^{-2}(\ln\mathcal{N})^2+\Delta t),\ t_j\in\mathfrak{D}_t^{\mathcal{M}}.$$

The first term on the right hand side of (37) is the interpolation error. Suppose $4\rho_1\in[x_i,x_{i+1}]$. Then, we use the following interpolation estimates

$$|(y_n-\mathcal{I}_jy_n)(4\rho_1,t_j)| \le Ch_\ell^2\left\|\partial_x^2y_n(.,t_j)\right\|_{L^\infty([x_i,x_{i+1}])},$$
$$|(y_n-\mathcal{I}_jy_n)(4\rho_1,t_j)| \le \left\|y_n(.,t_j)\right\|_{L^\infty([x_i,x_{i+1}])},\ n=1,2,$$

and the arguments in Lemma 4.2 to prove that

$$|(\boldsymbol{y}-\mathcal{I}_j\boldsymbol{y})(4\rho_1,t_j)| \le \boldsymbol{C}\mathcal{N}^{-2}(\ln\mathcal{N})^2.$$

Consequently,

$$\xi_{4\rho_1} \le C(\mathcal{N}^{-2}(\ln\mathcal{N})^2+\Delta t).$$

Similarly, we can prove that

$$\xi_{4\rho_2-3\rho_1} \le C(\mathcal{N}^{-2}(\ln\mathcal{N})^2+\Delta t).$$

On combining these error bounds, we get $\lambda \le C(\mathcal{N}^{-2}(\ln\mathcal{N})^2+\Delta t)$. Further, we have $\xi^1\le C$, since $||\boldsymbol{y}||_{L^\infty(\overline{\Omega})}\le C$. Hence,

$$||\widetilde{\mathbf{Y}}-\mathbf{Y}^k||_{L^\infty(\overline{\Omega}^{\mathcal{N},\mathcal{M}})} \le C\left(\frac{1}{2}\right)^k + C(\mathcal{N}^{-2}(\ln\mathcal{N})^2+\Delta t).$$

□

Theorem 4.5. *Suppose $\boldsymbol{y}$ and $\boldsymbol{Y}^k$ are the solutions of problem (2) and the proposed algorithm respectively. Then*

$$||\boldsymbol{y}-\mathbf{Y}^k||_{L^\infty(\overline{\Omega}^{\mathcal{N},\mathcal{M}})} \le C\left(\frac{1}{2}\right)^k + C(\mathcal{N}^{-2}(\ln\mathcal{N})^2+\Delta t). \tag{38}$$

Proof. The proof of the theorem can be obtained by combining Lemma 4.2 and Theorem 4.4 with (16). □

5. Numerical Experiments

To verify the theoretical findings given in the previous sections, we consider some Gierer-Meinhardt type test problems in this section. All experiments are performed on a Windows 10(64 bit) PC-Intel(R) Core(TM) i5-4200U CPU @1.60GHz, 6.00GB of RAM using MATLAB 2019a. The user defined threshold is chosen to be $\tau = \mathcal{N}^{-2}(\ln\mathcal{N})^2$ for $||\mathbf{Y}^{k+1}-\mathbf{Y}^k||_{L^\infty(\overline{\Omega}^{\mathcal{N},\mathcal{M}})}\le\tau$. Next, we define the algorithm that will be used to compute the numerical results.

$$[\boldsymbol{\mathcal{L}}_p^{\mathcal{N},\mathcal{M}}\mathbf{Y}_p]_{i,j} := [\delta_t^-\mathbf{Y}_p]_{i,j} - \boldsymbol{\varepsilon}[\delta_x^2\mathbf{Y}_p]_{i,j} + \boldsymbol{f}(x_i,t_j,[\mathbf{Y}_p]_{i,j}) = \mathbf{0}. \tag{39}$$

Example 5.1. Consider Gierer-Meinhardt system (2) with the following nonlinear reaction term and initial/boundary conditions

$$f_1(x,t,\boldsymbol{y}) = 3y_1-2y_2+t^2(\exp(-y_1^2)+\sin(y_2))+t(1-\exp(3t))\sin(\pi x),$$
$$f_2(x,t,\boldsymbol{y}) = -t^2y_1\left(1+\frac{1}{1+y_1^2}\right)+3y_2-10t^2(1-\cos(2\pi x)),$$

Algorithm: Schwarz waveform relaxation algorithm

Step 1. Initialize $\mathbf{Y}^0$ with $\mathbf{Y}^0(x_i,t_j)=\mathbf{0},\ (x_i,t_j)\in(0,1)\times(0,\mathcal{T}]$, $\mathbf{Y}^0(x_i,t_j)=\boldsymbol{y}(x_i,t_j)\ (x_i,t_j)\in\overline{\mathfrak{D}}^{\mathcal{N}}\times\{0\}$ and $\mathbf{Y}^0(x_i,t_j)=\boldsymbol{y}(x_i,t_j),\ (x_i,t_j)\in\{0,1\}\times\mathfrak{D}_t^{\mathcal{M}}$. Set $k=1$.

Step 2. Calculate $\mathbf{Y}_L^k$ using equation (11) and $\mathbf{Y}_R^k$ using equation (12). Next, calculate $\mathbf{Y}_r^k$ using equation (13) and $\mathbf{Y}_\ell^k$ using equation (14). Finally, calculate $\mathbf{Y}_m^k$ using equation (15).

Step 3. Update $\mathbf{Y}^k$ using (10).

Step 4. The final solution, $\mathbf{Y}^k$, is obtained if the stopping condition is achieved; if not, set $k=k+1$, and proceed to Step 2.

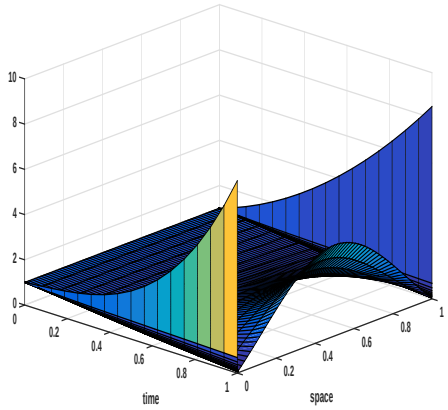

FIGURE 2. Solution component y_1 with Scheme 1 for Example 5.1 with $\varepsilon_1=10^{-7},\varepsilon_2=10^{-5}$ and $\mathcal{N}=64,\mathcal{M}=16$.

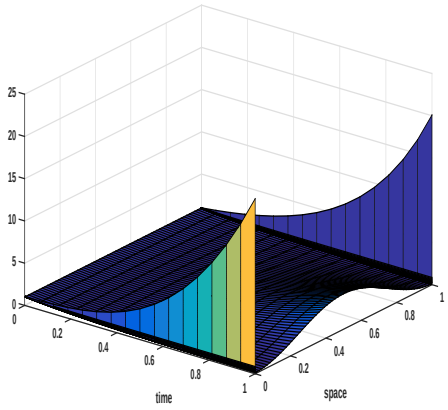

FIGURE 3. Solution component y_2 with Scheme 1 for Example 5.1 with $\varepsilon_1=10^{-7},\varepsilon_2=10^{-5}$ and $\mathcal{N}=64,\mathcal{M}=16$.

TABLE 1. Uniform errors $\mathbf{E}^{\mathcal{N},\Delta t}$ and uniform convergence rate $\boldsymbol{\mathcal{R}}^{\mathcal{N},\Delta t}$ for Example 5.1.

Schemes		$\mathcal{N}=2^5$ $\mathcal{M}=4$	$\mathcal{N}=2^6$ $\mathcal{M}=4^2$	$\mathcal{N}=2^7$ $\mathcal{M}=4^3$	$\mathcal{N}=2^8$ $\mathcal{M}=4^4$	$\mathcal{N}=2^9$ $\mathcal{M}=4^5$
Scheme 1	$E_1^{\mathcal{N},\Delta t}$	5.8467e-01	1.3635e-01	3.2901e-02	8.1412e-03	2.0121e-03
	$\mathcal{R}_1^{\mathcal{N},\Delta t}$	2.100	2.051	2.015	2.014	
	$E_2^{\mathcal{N},\Delta t}$	3.0848e-01	8.4248e-02	2.1595e-02	5.4327e-03	1.3241e-03
	$\mathcal{R}_2^{\mathcal{N},\Delta t}$	1.872	1.964	1.991	2.036	
Scheme 2	$E_1^{\mathcal{N},\Delta t}$	6.1280e-01	1.4884e-01	3.6471e-02	9.0623e-03	2.2620e-03
	$\mathcal{R}_1^{\mathcal{N},\Delta t}$	2.028	2.042	2.029	2.002	
	$E_2^{\mathcal{N},\Delta t}$	5.9452e-01	1.5039e-01	3.7589e-02	9.3952e-03	2.3471e-03
	$\mathcal{R}_2^{\mathcal{N},\Delta t}$	1.983	2.000	2.000	2.000	
Scheme (39)	$E_1^{\mathcal{N},\Delta t}$	6.8887e-01	1.8494e-01	4.6807e-02	1.1732e-02	2.8928e-03
	$\mathcal{R}_1^{\mathcal{N},\Delta t}$	1.897	1.982	1.996	2.019	
	$E_2^{\mathcal{N},\Delta t}$	7.0525e-01	1.7203e-01	4.2581e-02	1.0608e-02	2.6388e-03
	$\mathcal{R}_2^{\mathcal{N},\Delta t}$	2.035	2.014	2.004	2.007	

$$\boldsymbol{\varphi}_0(t) = (8t^3 - 1.5t^2 + t + 1, 20t^3 + \exp(t) - 2t^2)^T,\ \boldsymbol{\varphi}_1(t) = (4.5t^2 + 3t + 1, \exp(3t))^T,$$
$$\boldsymbol{\phi}(x) = (1,1)^T,\ \mathcal{T} = 1.$$

TABLE 2. Present algorithm with Scheme (39): Iteration counts with $\varepsilon_1 = 10^{-9}$ for Example 5.1.

$\varepsilon_2 = 10^{-q}$	$\mathcal{N}=2^5$ $\mathcal{M}=4$	$\mathcal{N}=2^6$ $\mathcal{M}=4^2$	$\mathcal{N}=2^7$ $\mathcal{M}=4^3$	$\mathcal{N}=2^8$ $\mathcal{M}=4^4$	$\mathcal{N}=2^9$ $\mathcal{M}=4^5$
$q=1$	4	5	6	6	7
2	3	3	5	5	6
3	3	3	4	5	5
4	3	3	4	5	4
5	3	3	3	4	4
6	3	3	3	3	3
7	2	2	2	2	3
8	2	2	2	2	2
9	2	2	2	2	2
10	1	1	1	1	1

We use the following double mesh method [38] to compute the maximum pointwise errors because the actual solution to this test problem is unknown. Further, the nonlinear discrete systems are solved by Newton's method, setting τ as the tolerance. We compute

$$\mathbf{E}^{\mathcal{N},\Delta t}_{\varepsilon_1,\varepsilon_2} = ||\mathbf{Y}^{\mathcal{N},\Delta t} - \mathbf{Y}^{2\mathcal{N},\Delta t/4}||_{L^\infty(\overline{\Omega}^{\mathcal{N},\mathcal{M}})},$$

where the approximation $\mathbf{Y}^{2\mathcal{N},\Delta t/4}$ is obtained by taking $2\mathcal{N}+1$ discretization points in x direction and $\Delta t/4$ mesh width in t direction by utilizing the same transition parameters ρ_1 and ρ_2 as for the solution $\mathbf{Y}^{\mathcal{N},\Delta t}$. The uniform errors $\mathbf{E}^{\mathcal{N},\Delta t}$ are calculated as

$$\mathbf{E}^{\mathcal{N},\Delta t} = \max_{\varepsilon_1} \mathbf{E}^{\mathcal{N},\Delta t}_{\varepsilon_1},$$

TABLE 3. Present algorithm with Scheme 1 or Scheme 2 : Iteration counts with $\varepsilon_1 = 10^{-9}$ for Example 5.1.

$\varepsilon_2 = 10^{-q}$	$\mathcal{N} = 2^5$ $\mathcal{M} = 4$	$\mathcal{N} = 2^6$ $\mathcal{M} = 4^2$	$\mathcal{N} = 2^7$ $\mathcal{M} = 4^3$	$\mathcal{N} = 2^8$ $\mathcal{M} = 4^4$	$\mathcal{N} = 2^9$ $\mathcal{M} = 4^5$
$q = 1$	4	5	5	6	6
2	3	3	4	4	5
3	3	3	3	4	4
4	3	3	4	3	4
5	3	3	3	4	4
6	3	3	3	3	4
7	2	2	2	2	3
8	2	2	2	2	2
9	2	2	2	2	2
10	1	1	1	1	1

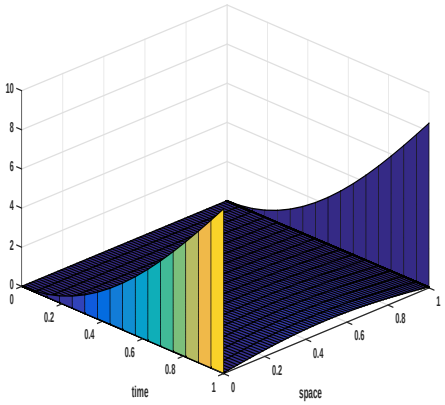

FIGURE 4. Component 1 with Scheme 2 for Example 5.2 with $\varepsilon_1 = 10^{-7}, \varepsilon_2 = 10^{-5}$ and $\mathcal{N} = 64, \mathcal{M} = 16$.

where $\mathbf{E}^{\mathcal{N},\Delta t}_{\varepsilon_1} = \max\{\mathbf{E}^{\mathcal{N},\Delta t}_{\varepsilon_1,1}, \mathbf{E}^{\mathcal{N},\Delta t}_{\varepsilon_1,10^{-1}}, ..., \mathbf{E}^{\mathcal{N},\Delta t}_{\varepsilon_1,10^{-s}}\}$ is calculated for a constant value of $\varepsilon_1 = 10^{-s}$, $s \in \{q : 0 \leq q \leq 10\}$. Next, we use the formula below to define the uniform convergence rates

$$\boldsymbol{\mathcal{R}}^{\mathcal{N},\Delta t} = \log_2(\mathbf{E}^{\mathcal{N},\Delta t}/\mathbf{E}^{2N,\Delta t/4}),$$

where $\boldsymbol{\mathcal{R}}^{\mathcal{N},\Delta t} = (\mathcal{R}_1^{\mathcal{N},\Delta t}, \mathcal{R}_2^{\mathcal{N},\Delta t})^T$ and $\mathbf{E}^{\mathcal{N},\Delta t} = (E_1^{\mathcal{N},\Delta t}, E_2^{\mathcal{N},\Delta t})^T$.

We also compute the numerical results using the algorithm with the standard discretization scheme, which uses the backward Euler method on a uniform mesh in time and the central difference scheme on a uniform mesh in space, as defined below

The solution plots for Examples 5.1 and 5.2 are displayed in Figures 2 - 3 and 4 -5. For Scheme 1, Scheme 2, and Scheme (39), the uniform errors and uniform convergence rates for the solution components are presented in Table 1 for Example 5.1. The numerical results presented in Table 1 are almost similar for all three schemes. Tables 2 and 3 display the number of iterations to achieve the stopping

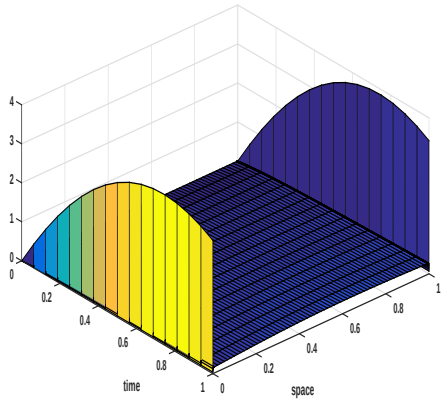

FIGURE 5. Solution Component y_2 with Scheme 2 for Example 5.2 with $\varepsilon_1 = 10^{-7}, \varepsilon_2 = 10^{-5}$ and $\mathcal{N} = 64, \mathcal{M} = 16$.

TABLE 4. Uniform errors $\mathbf{E}^{\mathcal{N},\Delta t}$ and uniform convergence rates $\boldsymbol{\mathcal{R}}^{\mathcal{N},\Delta t}$ for Example 5.2.

Schemes		$\mathcal{N} = 2^5$ $\mathcal{M} = 1/4$	$\mathcal{N} = 2^6$ $\mathcal{M} = 4^2$	$\mathcal{N} = 2^7$ $\mathcal{M} = 4^3$	$\mathcal{N} = 2^8$ $\mathcal{M} = 4^4$	$\mathcal{N} = 2^9$ $\mathcal{M} = 4^5$
Scheme 1	$E_1^{\mathcal{N},\Delta t}$	1.2734e-02	3.9623e-03	1.0423e-03	2.6382e-04	6.6120e-05
	$\mathcal{R}_1^{\mathcal{N},\Delta t}$	1.684	1.927	1.982	1.996	
	$E_2^{\mathcal{N},\Delta t}$	3.5016e-02	9.5811e-03	2.5464e-03	7.0867e-04	1.8222e-04
	$\mathcal{R}_2^{\mathcal{N},\Delta t}$	1.869	1.912	1.845	1.959	
Scheme 2	$E_1^{\mathcal{N},\Delta t}$	1.1026e-02	3.3801e-03	9.1004e-04	2.3167e-04	5.7932e-05
	$\mathcal{R}_1^{\mathcal{N},\Delta t}$	1.706	1.893	1.973	1.999	
	$E_2^{\mathcal{N},\Delta t}$	2.0197e-02	7.8078e-03	2.4604e-03	6.0747e-04	1.5148e-04
	$\mathcal{R}_2^{\mathcal{N},\Delta t}$	1.371	1.666	2.018	2.001	
Scheme (39)	$E_1^{\mathcal{N},\Delta t}$	1.4421e-02	4.8217e-03	1.3339e-03	3.4251e-04	8.6492e-05
	$\mathcal{R}_1^{\mathcal{N},\Delta t}$	1.581	1.854	1.959	1.985	
	$E_2^{\mathcal{N},\Delta t}$	1.9394e-02	7.9896e-03	2.6077e-03	6.9169e-04	1.7736e-04
	$\mathcal{R}_2^{\mathcal{N},\Delta t}$	1.279	1.615	1.915	1.963	

criterion. The number of iterations for the proposed algorithm with Scheme 1 and Scheme 2 are the same, whereas these counts are slightly different for Scheme (39).

Example 5.2. Consider the nonlinear coupled system (2) of singularly perturbed nature with the following nonlinear reaction term and initial/boundary conditions

$$f_1(x,t,\boldsymbol{y}) = 4y_1 - y_2 + \cos(y_2) - 2t(x - x^2 + \sin(\pi x)) - 4,$$
$$f_2(x,t,\boldsymbol{y}) = -y_1 - \sin(y_1) + 7y_2 + \sin^2(y_2) - xt - 1,$$
$$\boldsymbol{\varphi}_0 = (10t\sin t, 10\cos t(1-\exp(-t)))^T,\ \boldsymbol{\varphi}_1 = (10t\sin t, 10\cos t(1-\exp(-t)))^T,$$
$$\boldsymbol{\phi}(x) = (0,0)^T,\ \mathcal{T} = 1.$$

The uniform convergence rates $\boldsymbol{\mathcal{R}}^{\mathcal{N},\Delta t}$ and uniform errors $\mathbf{E}^{\mathcal{N},\Delta t}$ are computed in the same manner as before. The uniform errors and uniform convergence rates

TABLE 5. Present algorithm with Scheme (39): Iteration counts taking $\varepsilon_1 = 10^{-9}$ in Example 5.2.

$\varepsilon_2 = 10^{-q}$	$\mathcal{N} = 2^5$ $\mathcal{M} = 4$	$\mathcal{N} = 2^6$ $\mathcal{M} = 4^2$	$\mathcal{N} = 2^7$ $\mathcal{M} = 4^3$	$\mathcal{N} = 2^8$ $\mathcal{M} = 4^4$	$\mathcal{N} = 2^9$ $\mathcal{M} = 4^5$
$q = 1$	5	5	6	6	7
2	4	4	5	5	6
3	3	4	4	5	5
4	3	4	4	4	4
5	3	3	4	4	3
6	3	3	3	3	3
7	2	2	2	2	2
8	2	2	2	2	2
9	2	2	2	2	2
10	1	1	1	1	1

TABLE 6. Present algorithm with Scheme 1 or Scheme 2 : Iteration counts with $\varepsilon_1 = 10^{-9}$ in Example 5.2.

$\varepsilon_2 = 10^{-q}$	$\mathcal{N} = 2^5$ $\mathcal{M} = 4$	$\mathcal{N} = 2^6$ $\mathcal{M} = 4^2$	$\mathcal{N} = 2^7$ $\mathcal{M} = 4^3$	$\mathcal{N} = 2^8$ $\mathcal{M} = 4^4$	$\mathcal{N} = 2^9$ $\mathcal{M} = 4^5$
$q = 1$	4	5	6	6	6
2	3	4	4	5	5
3	3	4	4	4	5
4	3	3	4	4	4
5	3	3	3	4	3
6	3	3	3	3	3
7	2	2	2	2	3
8	2	2	2	2	2
9	2	2	2	2	2
10	1	1	1	1	1

for the Scheme 1, Scheme 2, and Scheme (39) for the solution components are presented in Table 4 for Example 5.2. Further, Tables 5 and 6 show how many iterations are necessary to satisfy the stopping constraint. Here, we also observe the same behavior of the numerical results as in Example 5.1.

TABLE 7. CPU time (in seconds) used by the present algorithm for Example 5.1 with $\varepsilon_1 = 10^{-7}$, $\varepsilon_2 = 10^{-5}$.

Scheme	$\mathcal{N} = 2^5$ $\mathcal{M} = 4^2$	$\mathcal{N} = 2^6$ $\mathcal{M} = 4^3$	$\mathcal{N} = 2^7$ $\mathcal{M} = 4^4$	$\mathcal{N} = 2^8$ $\mathcal{M} = 4^5$	$\mathcal{N} = 2^9$ $\mathcal{M} = 4^6$
Scheme 1	0.434	2.610	26.878	271.484	6854.164
Scheme 2	0.569	2.824	28.986	291.506	7086.662
Scheme (39)	1.064	4.095	57.706	933.209	46471.232

To show the efficiency of the algorithm with Schemes 1 and 2, we compare the computational cost required by the the algorithm with Schemes 1, 2, and Scheme (39) in Tables 7 and 8 for the Examples 5.1 and 5.2 respectively. These results

TABLE 8. CPU time (in seconds) used by the present algorithm for Example 5.2 with $\varepsilon_1 = 10^{-7}$, $\varepsilon_2 = 10^{-5}$.

Scheme	$\mathcal{N} = 2^5$ $\mathcal{M} = 4^2$	$\mathcal{N} = 2^6$ $\mathcal{M} = 4^3$	$\mathcal{N} = 2^7$ $\mathcal{M} = 4^4$	$\mathcal{N} = 2^8$ $\mathcal{M} = 4^5$	$\mathcal{N} = 2^9$ $\mathcal{M} = 4^6$
Scheme 1	0.895	2.198	18.481	209.241	5821.146
Scheme 2	0.783	2.856	20.185	249.665	6056.191
Scheme (39)	1.377	3.765	52.840	1066.341	42924.251

TABLE 9. Uniform errors $\mathbf{E}^{\mathcal{N},\Delta t}$ and uniform convergence rates $\boldsymbol{\mathcal{R}}^{\mathcal{N},\Delta t}$ using the tolerance $\tau = 10^{-7}$ for Example 5.2.

Schemes		$\mathcal{N} = 2^5$ $\mathcal{M} = 1/4$	$\mathcal{N} = 2^6$ $\mathcal{M} = 4^2$	$\mathcal{N} = 2^7$ $\mathcal{M} = 4^3$	$\mathcal{N} = 2^8$ $\mathcal{M} = 4^4$	$\mathcal{N} = 2^9$ $\mathcal{M} = 4^5$
Scheme 1	$E_1^{\mathcal{N},\Delta t}$	1.2734e-02	3.9623e-03	1.0423e-03	2.6382e-04	6.6159e-05
	$\mathcal{R}_1^{\mathcal{N},\Delta t}$	1.684	1.927	1.982	1.995	
	$E_2^{\mathcal{N},\Delta t}$	3.5016e-02	9.5811e-03	2.5347e-03	7.0668e-04	1.8916e-04
	$\mathcal{R}_2^{\mathcal{N},\Delta t}$	1.869	1.918	1.843	1.901	
Scheme 2	$E_1^{\mathcal{N},\Delta t}$	1.1017e-02	3.3773e-03	9.0948e-04	2.3211e-04	5.8595e-05
	$\mathcal{R}_1^{\mathcal{N},\Delta t}$	1.706	1.893	1.970	1.986	
	$E_2^{\mathcal{N},\Delta t}$	2.0012e-02	7.7631e-03	2.4473e-03	6.8585e-04	1.8496e-04
	$\mathcal{R}_2^{\mathcal{N},\Delta t}$	1.366	1.665	1.835	1.890	
Scheme (39)	$E_1^{\mathcal{N},\Delta t}$	1.4421e-02	4.8217e-03	1.3339e-03	3.4430e-04	8.761e-05
	$\mathcal{R}_1^{\mathcal{N},\Delta t}$	1.581	1.854	1.954	1.971	
	$E_2^{\mathcal{N},\Delta t}$	1.9220e-02	7.9597e-03	2.5881e-03	7.2213e-04	1.9257e-04
	$\mathcal{R}_2^{\mathcal{N},\Delta t}$	1.272	1.621	1.841	1.907	

TABLE 10. CPU time (in seconds) used by the present algorithm for Example 5.2 with $\varepsilon_1 = 10^{-7}$, $\varepsilon_2 = 10^{-5}$, and the tolerance $\tau = 10^{-7}$.

Scheme	$\mathcal{N} = 2^5$ $\mathcal{M} = 4^2$	$\mathcal{N} = 2^6$ $\mathcal{M} = 4^3$	$\mathcal{N} = 2^7$ $\mathcal{M} = 4^4$	$\mathcal{N} = 2^8$ $\mathcal{M} = 4^5$	$\mathcal{N} = 2^9$ $\mathcal{M} = 4^6$
Scheme 1	1.827	5.820	35.504	380.224	5972.221
Scheme 2	1.607	7.224	36.336	428.854	6176.527
Scheme (39)	1.851	8.299	81.535	1155.001	44608.912

are calculated for fixed values $\varepsilon_1 = 10^{-7}$ and $\varepsilon_2 = 10^{-5}$ and different values of discretization parameters $\mathcal{N}$ and Δt. These results clearly show that the algorithm with Schemes 1 and 2 is computationally more efficient than Scheme (39).

We also compute the numerical results using a fixed tolerance of $\tau = 10^{-7}$ as the stopping criterion for the algorithm. These results are shown in Tables 9 to 12. From these tables, we observe that the uniform errors and convergence rates are consistent with the previous results. Additionally, the conclusions for the three schemes remain unchanged. However, when comparing Tables 8 and 10, we find that using the fixed tolerance $\tau = 10^{-7}$ as the stopping criterion results in higher CPU time compared to using the tolerance $\tau = \mathcal{N}^{-2}(\ln \mathcal{N})^2$.

TABLE 11. Present algorithm with Scheme 1 : Iteration counts with $\varepsilon_1 = 10^{-9}$ and the tolerance $\tau = 10^{-7}$ for Example 5.2.

$\varepsilon_2 = 10^{-q}$	$\mathcal{N} = 2^5$ $\mathcal{M} = 4$	$\mathcal{N} = 2^6$ $\mathcal{M} = 4^2$	$\mathcal{N} = 2^7$ $\mathcal{M} = 4^3$	$\mathcal{N} = 2^8$ $\mathcal{M} = 4^4$	$\mathcal{N} = 2^9$ $\mathcal{M} = 4^5$
$q = 1$	7	7	7	7	7
2	4	5	6	6	6
3	4	4	4	5	6
4	4	4	5	5	5
5	4	4	4	4	4
6	3	3	4	4	4
7	2	2	2	2	2
8	2	2	2	2	2
9	2	2	2	2	2
10	2	2	2	2	2

TABLE 12. Present algorithm with Scheme (39) : Iteration counts with $\varepsilon_1 = 10^{-9}$ and the tolerance $\tau = 10^{-7}$ for Example 5.2.

$\varepsilon_2 = 10^{-q}$	$\mathcal{N} = 2^5$ $\mathcal{M} = 4$	$\mathcal{N} = 2^6$ $\mathcal{M} = 4^2$	$\mathcal{N} = 2^7$ $\mathcal{M} = 4^3$	$\mathcal{N} = 2^8$ $\mathcal{M} = 4^4$	$\mathcal{N} = 2^9$ $\mathcal{M} = 4^5$
$q = 1$	8	8	8	8	8
2	6	7	7	8	8
3	5	6	6	6	7
4	5	5	5	6	6
5	5	5	5	5	5
6	4	4	4	4	5
7	2	2	3	3	3
8	2	2	2	2	2
9	2	2	2	2	2
10	2	2	2	2	2

6. Conclusions

We have proposed a domain decomposition algorithm to solve the semilinear coupled system of singularly perturbed Gierer-Meinhardt type parabolic problems. On each subdomain, a classical central difference scheme in space along with the splitting of components technique in time, is utilized. We have shown that the proposed algorithm is parameter uniform, with the accuracy of almost second order in space variable and one in time variable. To support the theoretical findings and show the efficiency of the proposed algorithm, we have included two nonlinear coupled system of test problems. It is also worth noting that Scheme 1 can be implemented in parallel.

Acknowledgments

The author Sunil Kumar would like to thank the Science and Engineering Research Board (SERB) for giving the research support grant CRG/2023/003228 for the present work. The author Pratibhamoy Das wanted to acknowledge the Science and Engineering Research Board, Government of India, through the Project

No. MTR/2021/000797 for supporting the present research. We would like to express our gratitude to the Editor for taking time to handle the manuscript and to anonymous referees whose constructive comments are very helpful for improving the quality of our paper.

References

[1] C. Hirsch, Numerical computation of internal and external flows: fundamentals of numerical discretization, John Wiley and Sons, Inc., 1988.
[2] A. M. Soane, M. K. Gobbert, T. I. Seidman, Numerical exploration of a system of reaction-diffusion equations with internal and transient layers, Nonlinear Analysis: Real World Applications 6 (5) (2005) 914-934.
[3] F. Veerman, A. Doelman, Pulses in a Gierer-Meinhardt equation with a slow nonlinearity, SIAM Journal on Applied Dynamical Systems 12 (1) (2013) 28-60.
[4] F. Veerman, Breathing pulses in singularly perturbed reaction-diffusion systems, Nonlinearity 28 (7) (2015) 2211.
[5] P. Das, An a posteriori based convergence analysis for a nonlinear singularly perturbed system of delay differential equations on an adaptive mesh, Numerical Algorithms 81 (2019) 465-487.
[6] R. Choudhary, S. Singh, P. Das, D. Kumar, A higher-order stable numerical approximation for time-fractional non-linear Kuramoto-Sivashinsky equation based on quintic B-spline, Mathematical Methods in the Applied Sciences 47 (2024) 11953-11975.
[7] S. Saini, P. Das, S. Kumar, Parameter uniform higher order numerical treatment for singularly perturbed Robin type parabolic reaction diffusion multiple scale problems with large delay in time, Applied Numerical Mathematics 196 (2024) 1-21.
[8] T. Kolokolnikov, J. Wei, M. Winter, Existence and stability analysis of spiky solutions for the Gierer-Meinhardt system with large reaction rates, Physica D 238 (2009) 1695-1710.
[9] D. Gomez, L. Mei, J. Wei, Boundary layer solutions in the Gierer-Meinhardt system with inhomogeneous boundary conditions, Physica D 429 (2022) 133071.
[10] H. M. Srivastava, A. K. Nain, R. K. Vats, P. Das, A theoretical study of the fractional-order p-Laplacian nonlinear Hadamard type turbulent flow models having the Ulam-Hyers stability, Revista de la Real Academia de Ciencias Exactas, Fisicas y Naturales. Serie A. Matematicas 117:160 (2023).
[11] S. C. S. Rao, A. K. Chaturvedi, Pointwise error estimates for a system of two singularly perturbed time-dependent semilinear reaction-diffusion equations, Mathematical Methods in the Applied Sciences 44 (17) (2021) 13287-13325.
[12] H.-G. Roos, M. Stynes, L. Tobiska, Robust numerical methods for singularly perturbed differential equations: convection-diffusion-reaction and flow problems, Vol. 24, Springer Science and Business Media, 2008.
[13] J. J. H. Miller, E. ORiordan, G. I. Shishkin, Fitted Numerical Methods for Singular Perturbation Problems, World Scientific, Singapore, 1996.
[14] S. Santra, J. Mohapatra, P. Das, D. Choudhuri, Higher order approximations for fractional order integro-parabolic partial differential equations on an adaptive mesh with error analysis, Computers and Mathematics with Applications 150 (2023) 87-101.
[15] V. Gupta, M. K. Kadalbajoo, A layer adaptive B-spline collocation method for singularly perturbed one-dimensional parabolic problem with a boundary turning point, Numerical Methods for Partial Differential Equations 27 (5) (2011) 1143-1164.
[16] V. Gupta, S. K. Sahoo, R. K. Dubey, Robust higher order finite difference scheme for singularly perturbed turning point problem with two outflow boundary layers, Computational and Applied Mathematics 40 (2021) 179.
[17] N. Sharma, A. K. Pani, K. K. Sharma, Expanded mixed FEM with lowest order RT elements for nonlinear and nonlocal parabolic problems, Advances in Computational Mathematics 44 (2018) 1537-1571.
[18] P. Mishra, K. K. Sharma, A. K. Pani, G. Fairweather, High-order discrete-time orthogonal spline collocation methods for singularly perturbed 1D parabolic reaction-diffusion problems, Numerical Methods for Partial Differential Equations 36 (3) (2020) 495-523.
[19] P. Mishra, K. K. Sharma, A. K. Pani, G. Fairweather, Orthogonal spline collocation for singularly perturbed reaction diffusion problems in one dimension, International Journal of Numerical Analysis and Modeling 16 (4) (2019) 647-667.

[20] J. B. Munyakazi, A uniformly convergent nonstandard finite difference scheme for a system of convection-diffusion equations, Computational and Applied Mathematics 34 (2015) 1153-1165.
[21] S. Saini, P. Das, S. Kumar, Computational cost reduction for coupled system of multiple scale reaction diffusion problems with mixed type boundary conditions having boundary layers, Revista de la Real Academia de Ciencias Exactas, Fisicas y Naturales. Serie A. Matematicas 117 (2023) 1-27.
[22] J. Liu, Y. Jiang, Waveform relaxation for reaction-diffusion equations, Journal of Computational and Applied Mathematics 235 (2011) 5040-5055.
[23] J. Singh, S. Kumar, A domain decomposition method of Schwarz waveform relaxation type for singularly perturbed nonlinear parabolic problems, International Journal of Computer Mathematics 100 (2023) 177 -191.
[24] S. Kumar, Aakansha, J. Singh, H. Ramos, Parameter-uniform convergence analysis of a domain decomposition method for singularly perturbed parabolic problems with robin boundary conditions, Journal of Applied Mathematics and Computing 69 (2) (2023) 2239-2261.
[25] M. Dehghan, F. Shakeri, The use of the decomposition procedure of adomian for solving a delay differential equation arising in electrodynamics, Physica Scripta 78 (2008) 065004.
[26] A. Toselli, O. Widlund, Domain Decomposition Methods-Algorithms and Theory, Springer Series in Computational Mathematics, Springer, 2010.
[27] I. Boglaev, Domain decomposition in boundary layers for singularly perturbed problems, Applied Numerical Mathematics 34 (2000) 145-166.
[28] E. Giladi, H. B. Keller, Space-time domain decomposition for parabolic problems, Numerische Mathematik 93 (2) (2002) 279-313.
[29] M. J. Gander, A. M. Stuart, Space-time continuous analysis of waveform relaxation for the heat equation, SIAM Journal of Scientific Computing 19 (1998) 2014-2031.
[30] M. Kamranian, M. Dehghan, M. Tatari, An image denoising approach based on a mesh-free method and the domain decomposition technique, Engineering Analysis with Boundary Elements 39 (2014) 101-110.
[31] D. S. Daoud, Overlapping Schwarz waveform relaxation method for the solution of the forwardbackward heat equation, Journal of Computational and Applied Mathematics 208 (2007) 380-390.
[32] M. J. Gander, C. Rohde, Overlapping Schwarz waveform relaxation for convection dominated nonlinear conservation laws, SIAM Journal of Scientific Computing 27 (2005) 415-439.
[33] S. Kumar, S. C. S. Rao, A robust overlapping schwarz domain decomposition algorithm for timedependent singularly perturbed reaction-diffusion problems, Journal of Computational and Applied Mathematics 261 (2014) 127-138.
[34] J. Singh, S. Kumar, M. Kumar, A domain decomposition method for solving singularly perturbed parabolic reaction-diffusion problems with time delay, Numerical Methods for Partial Differential Equations 34 (5) (2018) 1849-1866.
[35] G. I. Shishkin, L. P. Shishkina, Approximation of a system of semilinear singularly perturbed parabolic reaction-diffusion equations on a vertical strip, Journal of Physics: Conference Series 138 (1) (2008) 012026.
[36] L. Shishkina, G. Shishkin, Conservative numerical method for a system of semilinear singularly perturbed parabolic reaction-diffusion equations, Mathematical Modelling and Analysis 14 (2) (2009) 211-228.
[37] N. Madden, M. Stynes, A uniformly convergent numerical method for a coupled system of two singularly perturbed linear reaction-diffusion problems, IMA Journal of Numerical Analysis 23 (2003) 627-644.
[38] D. Shakti, J. Mohapatra, P. Das, J. Vigo-Aguiar, A moving mesh refinement based optimal accurate uniformly convergent computational method for a parabolic system of boundary layer originated reaction diffusion problems with arbitrary small diffusion terms, Journal of Computational and Applied Mathematics 404 (2022) 113167.

Department of Mathematical Sciences, Indian Institute of Technology (BHU) Varanasi, India
E-mail: aakansha.rs.mat18@itbhu.ac.in and skumar.iitd@gmail.com
URL: https://www.iitbhu.ac.in/dept/mat/people/skumarmat/

Department of Mathematics, Indian Institute of Technology Patna, India
E-mail: pratibhamoy@iitp.ac.in and pratibhamoy@gmail.com
URL: https://www.iitp.ac.in/people-dept-menu/faculty/263:view-profile-60